Geotechnical Engineering Journal of the SEAGS & AGSSEA Vol. 41 No.3 September 2010 ISSN 0046-5828

Recent Advances in Pile Testing and Diaphragm Wall Construction in Japan

Kenji Ishihara
Chuo University, Hachiōji, Tokyo, Japan
E-mail: kenji-ishihara@e-mail.jp

ABSTRACT: The first part of this paper consists of brief introduction of the in-situ pile loading tests that have been conducted in Japan over the last two decades in connection with the design and construction of high-rise buildings in areas of soft soil deposits. In addition to the conventional types of tests in which the load is applied at the top and at the toe of the pile (O-cell test), what may be called "pile toe bearing test" and "skin friction test" is introduced. The results of these tests are described and compared with those from the conventional type of the pile loading tests. In-situ prototype tests are also introduced in which bearing power of Barrette type pile is compared with that of the circular type pile. A special case of in-situ pile loading tests conducted in Singapore is also introduced in which the friction between the circular ring-shaped concrete segment and the surrounding soil deposit was measured directly during excavation of the shaft by applying loads up and down by jacks installed between two adjacent segments in vertical direction. The second part of this paper is a brief description on constructions of large-diameter circular diaphragm walls that was carried out about 10 years ago for the LNG storage tank in the coastal site in Tokyo Bay. The construction of the large-scale Kawasaki Island in the middle of Tokyo Bay in Japan will also be introduced. The whole scheme and process of construction is for these two undertakings is introduced with some comments on observed behaviour of the walls and on special precaution taken during construction.

1. INTRODUCTION

In the design and practice of foundations supporting heavy-weight structures such as high-rise buildings or large-scale facilities, of utmost importance is to know the load-carrying characteristics of soil or rock deposits at depths as deep as 30m-50m. Estimates of the load-bearing capacity for piles embedded into such deep-seated deposits have been made generally by carrying out what is known as the O-cell test or pile toe loading test. In some cases, direct loading tests are performed by large concrete blocks or segments on the intact surface of the deep deposits which are exposed during excavation of pits or shafts for foundation construction. The outcome of these in-situ tests has not unfortunately been publicized and compiled to the extent that these data can be effectively utilized for the design practice in the future. In view of this, some data from the in-situ pile loading tests performed in Japan were collected and presented in this paper.

It is to be noted that the soil deposit near the surface in the area of industry and mega city in Japan, is generally composed of soft soil of alluvial origin underlaid by alternative layers of stiff sand, clay, sand and gravel of diluvial origin. It is the generally adopted criterion that some of the stiff sand or gravel layer can be chosen as a bearing layer to support the piles. Thus, the end bearing type piles is frequently used in Japan rather than the friction type pile. However, since the stiff bearing layer is seated at great depths of about 20-50m, the O-cell tests have often been adopted to identify whether a given deposit is competent enough to mobilize the necessary bearing power. Some of the results of in-situ pile loading tests recently obtained in Japan by this method are introduced in this paper.

In the case of the deep-seated foundation supported by the diaphragm walls, the O-cell test is not applicable and some other methods need to be explored. In important projects, efforts have been made to measure directly the bearing power or skin friction within excavated pits or shafts by means of the plate loading tests performed on exposed surface of intact stiff sand, gravel and rocks. As one of the attempts in this context, an example of in-situ loading tests conducted in Singapore is introduced in this paper.

The other topics of importance in the foundation engineering would be the design and construction of the large-scale diaphragm wall, particularly when it is used as circular walls without any bracing. In the round–shaped walls, the hoop compression and its distribution in the circumferential direction are important factors to be considered with utmost precaution. The method of design and results of monitoring in this regard will be introduced by quoting an example of constructing a large LNG storage tank in Tokyo. When the circular wall is constructed under the seabed, one of the major concerns is the safety against the bottom heave and piping due to high hydraulic gradient of seepage water. These issues will be briefly touched on by quoting an example of the large scale construction of Kawasaki man-made island in the middle of Tokyo Bay in Japan.

Accumulation of in-situ data on pile testing is so much both in content and volume that it was difficult to overview all of them and come up with a state-of-the-art text from a fair point of view. What is written here is part of the test data which is considered appropriate in the context of the present presentation. There are also many construction examples of circular diaphragm walls. Because of the limitation in several respects, it was not possible to prepare a comprehensive overview of the current state of the practice. However, it is believed that the main points of the current practice in Japan are understood via the typical examples introduced here.

2. PILE TOE LOADING TEST

2.1 General

The pile top loading test in which loads are applied directly on top of piles has long been the method commonly adopted to verify actual bearing capacity of piles in the field. When the size of piles is relatively small corresponding to a low magnitude of design load, this method proved to be the most practical and useful tool for assessing the load-carrying capacity of piles. However, the demand for greater bearing power has increased in recent years in unison with increasing size and weight of buildings and facilities. Thus, required size and embedment depth of piles have increased remarkably. In such situations, the top loading test has become no longer recognized as an effective means to evaluate in-situ performance of large piles,
because it requires large trestles and facilities on the ground surface to apply heavy weight to the pile head, and therefore becomes expensive.

To cope with this, what is called pile toe loading test has become a commonly used procedure. This method consists of applying up and down forces at the tip of piles by means of a large jack which has been embedded in advance at the pile toe. In its original form proposed by Osterberg in 1984 for bored piles, a flat pancake-like cell was placed at the bottom of the drilled shaft before the concrete was poured. After the concrete has cured, the cell was pressurized internally by oil pressure, creating an upward force on the shaft and simultaneously an equal magnitude of force downwards to the bottom of the shaft. The downward

force to monitor bearing power of the pile toe is resisted by the upward force mobilized by the friction on the surface of the pile body. At the same time, it is possible to monitor the shaft friction as well while the reaction is taken by the downward directed bearing power. The mutually counteracting forces as above are utilized to apply two major forces, that is, for the end bearing test and also for the shaft resistance test. The upward movements of the pile at its toe and downward displacement of the ground at the pile toe can be measured independently via the two long bars with their ends attached through the pipes to the top and bottom of the pressurized jack. Thus, the upward displacement of the shaft is known along with the downward movement of the pile toe, thereby permitting the load-displacement relation to be established for the shaft resistance as well as the end bearing power.

The advantages of using this technique are summarized as follows:

1) There is no need to provide large equipments such as heavy weights or reaction piles on the ground surface for applying the force on the pile top, making it easier and inexpensive to install the test setup. The oil pump and several ancillary guages for monitoring pressure and displacements are the only major apparatus for the test setup on the ground surface which are simple and installed in a limited space.
2) As far as the end bearing is concerned, the ultimate value is measured directly, as a load of high intensity can be applied just to the soil deposit adjacent to the pile toe.

The above method, as referred to as "O-cell test" has been used widely for evaluating the in-situ performance characteristics of large and long piles. In Japan, the original setup was modified to some extent particularly in the mechanical part for applying the pressure at the pile toe. Instead of the pressure cell, a mechanical system consisting of a large-capacity jack at the pile toe and the measuring device controlled on the ground surface have been incorporated and in common use for carrying out the pile loading tests. The test setup of general use in Japan for the O-cell tests is schematically illustrated in Fig. 1.

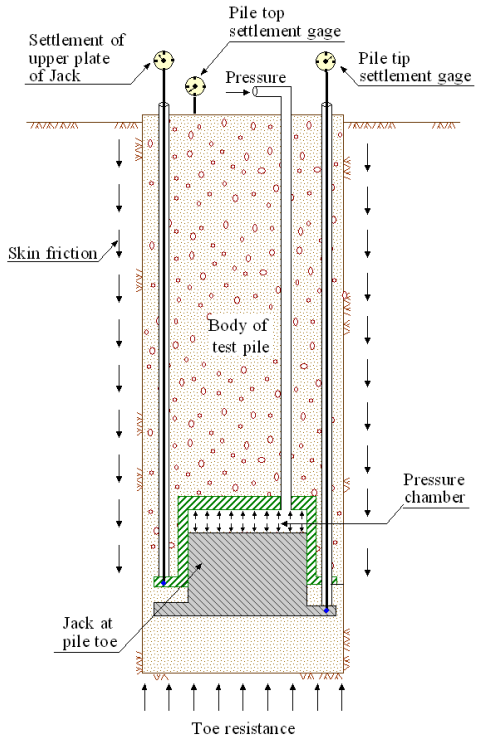

Figure 1. Schematic diagram for pile toe loading test (Ogura et al. 1997)

2.2 Pile Toe Loading Test at Kanto Postal Bureu Site

Taking advantage of the construction of the new 28-storey building for the postal bureau office in Saitama Prefecture due north of Tokyo, a series of pile tip loading tests was conducted by Shibuya et al. (1997) to assess the end bearing capacity of cast-in-place reinforced concrete piles. The building was 129.8 high and had two-storey basements. The site is located at the northern part of Ohmiya terrace area and consists of a series of soil layers of diluvial origin, as displayed in Fig. 2. Below the surface fill, there exists a dense sand deposit underlaid by silty clay with a SPT N-value of about 5. Below this deposit, a thick dense sand deposit with N>50 was shown to exist at depths between 45m and 60m, which was considered competent enough to act as an end-bearing layer of the piles.

To substantiate its bearing capacity, a jack 1.3m in diameter and 1.044m high with a movement stroke of 50cm was embedded at the pile toe through the procedure as illustrated in Fig. 3. In the present case, a hole with a diameter of 2.2m was drilled to a depth of 48m. After cleaning the bottom, a hopper laded with cement-mortar was lowered through the mud water to provide a sound base for the pile toe and then the jack-attached reinforcement cage was lowered so that the jack could be made to sit at the right position of the base. Concrete was then poured to form the test pile. The area of cross section at the pile tip was Ap=3.8m^2. After curing for 34days, the load was applied cyclically to the jack. One of the results of the pile toe loading tests is demonstrated in Fig. 4. Shown in Fig. 4(b) are the settlements, Sp, plotted versus the load, Pp, both monitored at the pile tip. It is known that the ultimate value of the end bearing is about 30MN and this is mobilized when the pile tip was displaced by 50cm. The effective nominal bearing capacity is normally defined in Japan as the load intensity at the stage when the pile is displaced by an amount equal to 10% of the diameter of the pile tip.

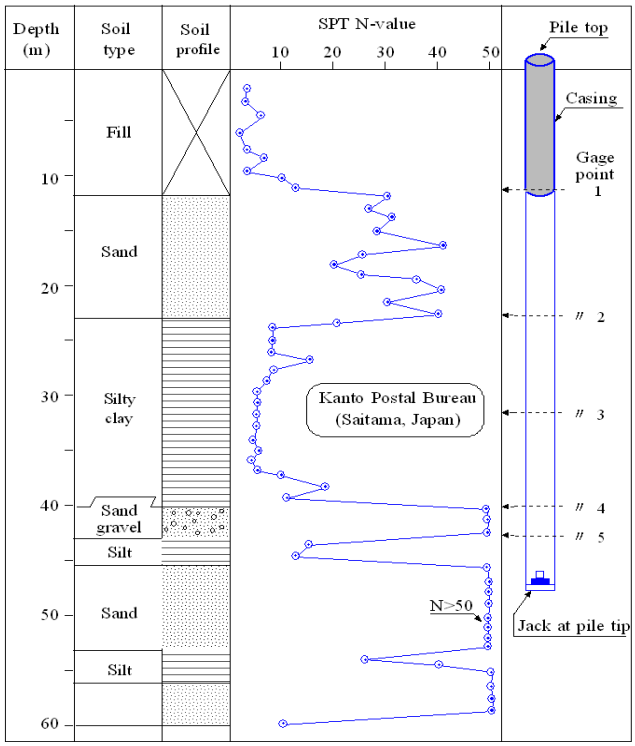

Figure 2. Soil profile at the site of Kanto Postal Bureau (Shibuya et al. 1997)

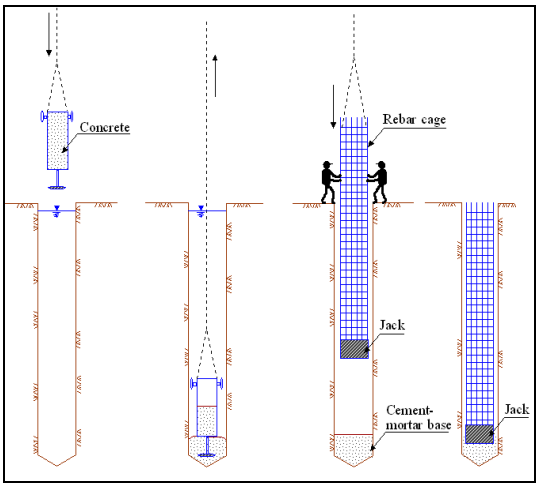

Figure 3. Procedures for installing a jack at the toe of the cast-in-place reinforced concrete pile

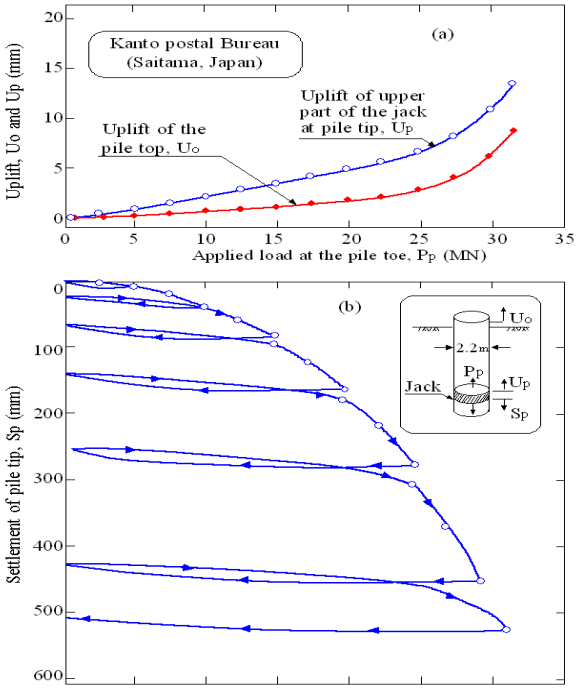

Figure 4. Results of the pile toe loading test at the site of Kanto Postal Bureau (Shibuya et al. 1997)

In this case, by reading off a value of 23MN corresponding to the settlement of 10% of the pile diameter, the nominal bearing capacity was estimated as 23MN/3.8 m² = 6.05MN/m² = 605t/m². In this particular test, values of upward movement of the pile top, Uo, was also monitored on the ground surface. The measured uplifts at the top, Uo, and at the pile tip, Up, are shown in Fig. 4(a) as plots versus the load, Pp, applied at the pile tip. It can be seen that the amount of uplift at the pile tip is greater than that at the pile top indicating the fact that the pile body tended to shrink due to the compressive load.

To monitor the friction along the shaft, the strain gages were pasted on the reinforcement at five depths as indicated in Fig. 2. By reading the compressive strains of the gages, it was possible to calculate the total magnitude of the vertical load being applied to the cross sections at each of the five depths. The axial load distributions thus obtained through the depth are displayed in Fig. 5 where it is noticed that the reduction in the axial load between two neighboring points of measurement is taken over by the equal magnitude of friction acting on the surface of the pile body.

The frictional force intensity between two adjacent points of measurements thus calculated is shown in Fig. 6 as plots versus the displacement between these two points. It can be seen that the frictional force between the Section 1 and the top is almost equal to zero indicating that the friction was cut off by the presence of the casing as accordingly shown in Fig. 2. The friction between Section 4 and the jack at the pile tip is known to reach its maximum value of 20t/m^2 when it was fully mobilized. This value was almost equal to the friction of 17t/ m^2 which had been postulated when the design was made.

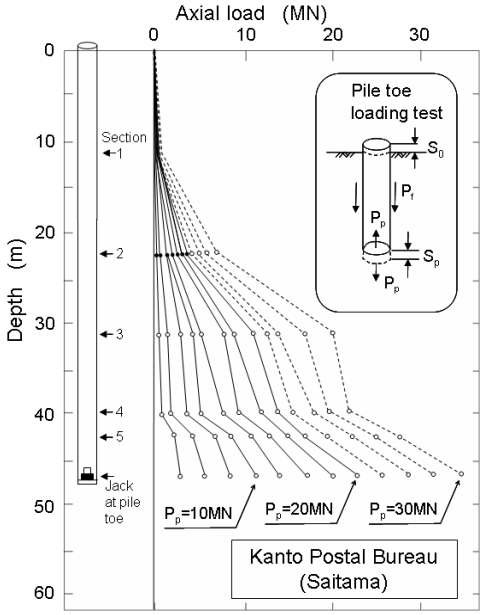

Figure 5. Axial load versus depth in the pile toe loading test at Kanto Postal Bureau (Shibuya et al. 1997)

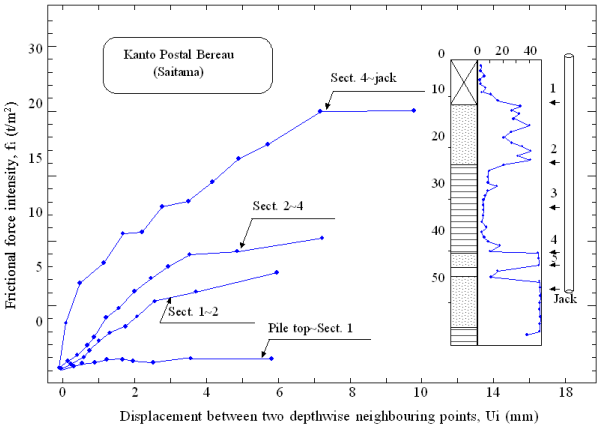

Figure 6. Frictional force intensity on the shaft versus the displacement of two neighbouring points (Shibuya et al. 1997)

2.3 Load-Settlement Curves at the Pile Top Estimated From the Pile Toe Loading Tests

The load-settlement relations, that is, Pp vs. Sp curves can be obtained in-situ with the optimum cost as described above but what is indeed necessary in the design of piles is the load-settlement relation, P_o vs. S_o curve at the top of piles. There are several models proposed to estimate the relation at the top based on the results of the pile toe loading test. One of them is what is termed "Load transfer method" proposed by Kishida and Tsubakihara (1993). Using this method, the $P_o - S_o$ curve at the pile top at Kanto Postal Bureau site was evaluated based on the

$P_p - S_p$ relation which was represented by a hyperbolic curve. The result of the analysis is shown in Fig. 7, together with the original $P_p - S_p$ relation obtained from the pile toe loading test. It is noted that the ultimate value of the skin friction, that is, $P_f = 30MN$, which should be equal to the upward load at the pile toe, can be estimated directly from the test result corresponding to the settlement of 50cm.

The curve predicted by the model is seen shifting rightwards by an amount approximately equal to the toe resistance which was gradually mobilized with increasing settlement. There are many other cases of similar studies in which the $P_o - S_o$ curve predicted by the $P_p - S_p$ relation via the model shows a good coincidence with the $P_o - S_o$ relation actually measured at the pile top. Thus, it is now considered appropriate to perform the pile toe loading test and to estimate the $P_o - S_o$ curve at the pile top to be incorporated in the design.

2.4 Compiled Results of the Pile-Toe Loading Tests

There have been a majority of test data of similar nature ever performed in Japan at various sites to obtain the end bearing capacity of dense sand deposits and soft rocks. These were summarized by Ogura et al. (1998) as shown in Fig. 8 in terms of the load intensity at the pile toe, P_p / A_p, plotted versus the settlement, S_p, divided by the diameter of the pile D_p at the pile tip. It may be seen in Fig. 8 that the pile tip settlement is much smaller for soft rock and gravelly sands than that for sand deposits. This implies the fact that, for the stiff deposits generally considered competent; the end bearing capacity is greater in soft rock or gravelly sand deposits as compared to that in the dense sand deposits.

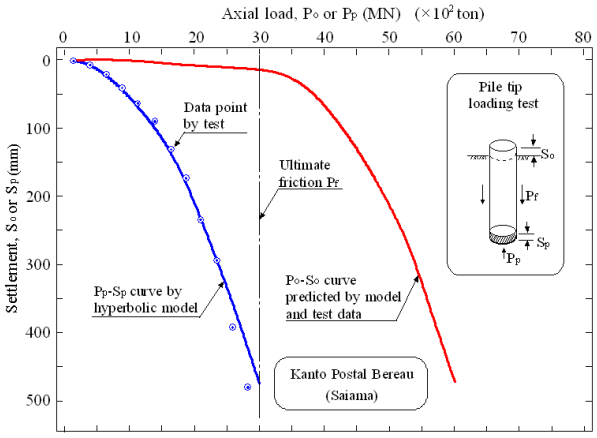

Figure 7. The load-settlement curve at the pile top estimated from the Pp-Sp relation by using the load transfer method (Shibuya et al. 1997)

3. PILE TOE BEARING TEST AND SHAFT RESISTANCE TEST

3.1 Concepts of the Pile Toe Bearing Test and Skin Friction Test

Shown in Fig. 9 are the illustrations for four types of pile loading tests ever performed. Figure 9(a) is the normal type of the pile top loading test. The pile toe loading test as described in the foregoing section is illustrated in Fig. 9(b). This test can be carried out to know the bearing capacity of the pile toe. However, there remains some influence in the vicinity of the pile tip, of reducing the vertical confining stress due to the shaft friction directed upwards. To eliminate this effect, if any, what is called "Pile toe bearing test" was proposed as illustrated in Fig. 9(c). In this type of test an axial load approximately equal to the upward force at the end jack is applied in addition at the pile top to discard the shaft friction. The magnitude of the force at the pile top is slightly smaller than the upward force from jack by an amount equal to the weight of the pile body. By means of this test, it is anticipated that the genuine value of end bearing capacity free from the influence of the shaft friction can be measured/obtained.

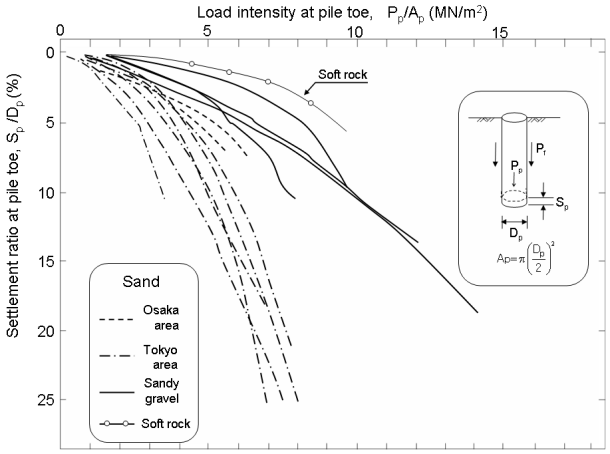

Figure 8. Summary of the pile toe loading tests (Ogura et al. 1998)

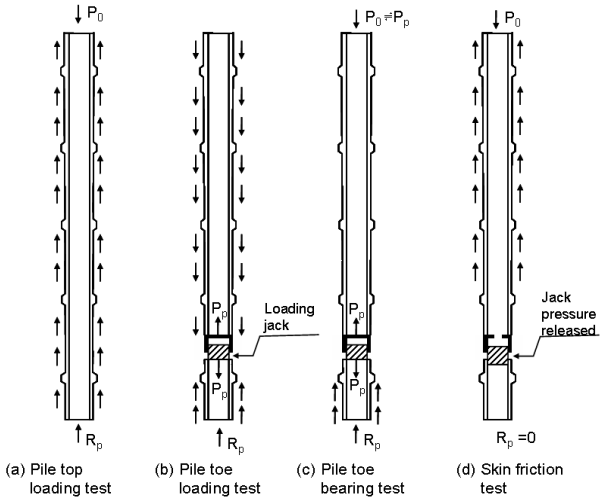

Figure 9. Four types of pile loading test

The fourth type of test is the one called "Skin-friction test". This type of test was proposed to cope with the criticism saying that in the widely used O-cell loading test, the frictional force along the shaft is mobilized in the downward direction which is opposite to the direction activated in the normal working conditions of in-situ piles. In an attempt to shed some light on this aspect, the skin friction test was developed by Dr. Ogura and his associates (2005). As illustrated in Fig. 9(d), this test consists of applying an axial force, first of all, at the pile top which is approximately equal to the upward force at the pile tip while the end-installed jack is in operation. Then, the pressure in jack is released. There is no force acting upward from the pile toe. Thus, the axial load, Po, applied at the pile top is totally resisted by the friction mobilized on the surface of the shaft. This is the principle of performing the skin friction tests.

3.2 Pile Toe Bearing Test and Skin Friction Tests at Kaifu Site in Aichi Prefecture

The test site is located at Kaifu near Nagoya where the deposits consist of a series of soil layers as shown in Fig. 10. The depths at which the jack was installed on two piles A and B are also indicated in Fig. 10. The site is located in the flood plain area composed of layers of soft silt and clay deposits with the SPT N-value of the order of 0 to 5. There exists a gravelly sand layer at the depth of 48.5m. Two precast concrete piles, denoted by A-pile and B-pile, were used for in-situ loading tests. The A-pile with a diameter of 1.0m was embedded to a depth of 42m where a 0.5m-height jack was installed. Below this depth, the pile was modulated through the 5m-length to a depth of 47.5m where a sand layer with N-value of 24 was encountered. For this modulated portion near the bottom, the diameter was 1.0m but for the non-modulated part the diameter was 80cm. The aim of the loading test by the A-pile was to know the toe bearing capacity of the sand deposit. The B-pile with a diameter of 0.8m was a straight pile to a depth of 44m where a 0.5m in height jack was attached. Below this, the modulated pile with the diameter of 1.0m was jointed downwards as illustrated in Fig. 10. The aim of the test by the B-pile was to examine the bearing power of the gravelly sand layer with a N-value of 60 at a depth of 49m.

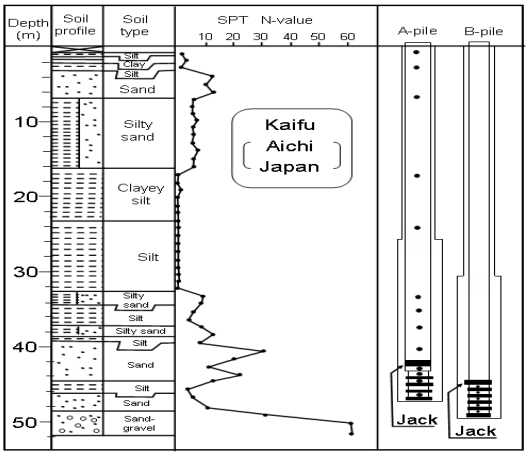

Figure 10 Soil profile at Kaifu site and embedment of two piles for toe bearing and skin friction tests (Ogura et al. 2005)

The prefabricated piles were installed in pre-bored holes after the bottom had been cleaned up. Milky cement was poured and churned with the soils at the bottom to prepare sound beds for placing the piles. After the piles were put in place, the cement mortar was poured to fill the annular space between the precast pile and the surrounding soils.

3.2.1 Pile Toe Bearing Test

The results of the pile toe bearing test on the A-pile is demonstrated in Fig. 11 in terms of the jack-applied load P_j plotted versus the downward displacement of the pile, S_j, at the point of the jack and also the displacement, Sp, at the pile tip. It can be seen in Fig. 11 that the displacement at the jack point is slightly larger than that at the pile tip. This is due to a slight compression of the pile body taking place through the 5m-long portion between the jack point and the pile tip. However, the load-settlement curves for the pile toe loading are, by and large, the same for the two plots of P_j versus S_j and Sp. It can also be seen in Fig. 11 that the ultimate bearing power of 10.87MN was achieved with a settlement of 17.6cm at the pile toe in the sand deposit of N=24 at the depth of 47m.

Measurements were made of the axial strains by means of strain gauges pasted to the reinforcement cage through the pile length as indicated by the dotted points on the right-hand side of Fig. 10. Over the portion of the pile from the top down to the jack point, the axial load monitored by the strain gages was shown to take approximately an identical value which is equal to $Po \cong Pp$. In the 5m-long portion from the jack point to the pile tip, the axial force as measured by the strain gages at five points is displayed in Fig. 12, where it can be seen that the axial load tends to decrease with increasing depth from the depth 42m to 47m due to the skin friction mobilized over the 5m long portion above the pile toe.

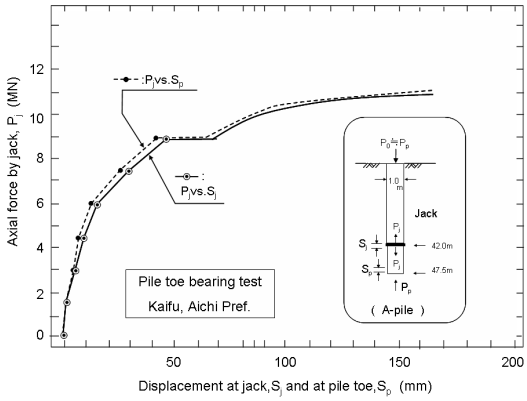

Figure 11. Load-displacement curves from the pile toe bearing test at Kaifu (Ogura et al. 2005)

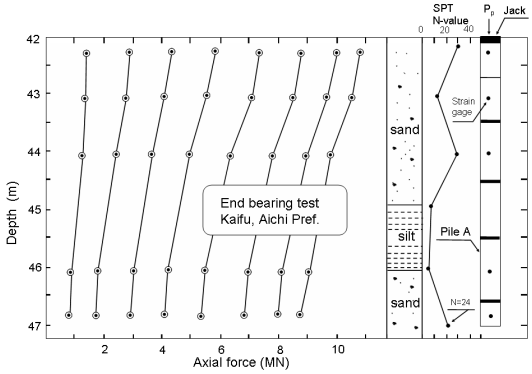

Figure 12. Load-displacement curves obtained from the pile toe bearing tests at Kaifu (Ogura et al. 2005)

3.2.2 Skin Friction Test

Following the toe bearing test on the A-pile, the skin friction test was carried out on the same pile by reducing the jack pressure while keeping the pile top load unchanged. The reduction in the jack pressure was assumed to be equivalent to the increase in the load P_o at the pile top which is regarded as indicating the corresponding increase in the skin friction R_d. The result of the test is displayed in Fig. 13 in terms of Po or R_d plotted versus the vertical displacement, S_o, at the pile top or S_j at jack point. It may be seen that, for a given axial load at pile top, the displacement at the jack point, S_j, is smaller than that at the pile top, indicating that this difference corresponds to the shortening of the pile body. The depth wise distribution of the axial load through the pile length as evaluated by the strain gage reading is displayed in Fig. 14. It can be seen that the maximum load, Po, at the top tended to decrease with depth and became equal to zero at the pile tip for all the steps of loading.

3.2.3 Comparison of the Toe Bearing Capacity between the Sand and Gravel Deposits

As demonstrated in Fig. 10, the B-pile was put in place in the sandy gravel layer at the depth of 49m where the SPT N-value was 60. The result of the pile toe bearing test conducted on the

B-pile are shown in Fig. 15 where the end bearing load intensity, q_p, as defined by $q_p = P_p / A_p$ is plotted versus the vertical displacement, S_j. at the jack point or at the pile tip, S_p. The result of the pile toe bearing test on the A-pile shown in Fig. 11 is also replotted in Fig. 15 in the same fashion for comparison. It is obvious from Fig. 15 that the end bearing load intensity q_p in the gravel is much higher than that in the sand deposit.

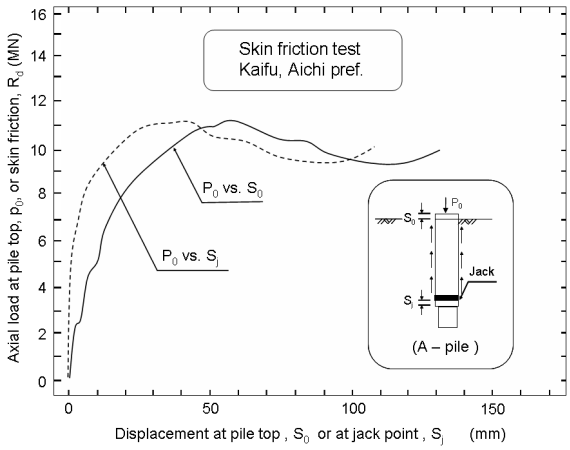

Figure 13. Skin friction distributions through the toe portion of A-pile (Ogura et al. 2005)

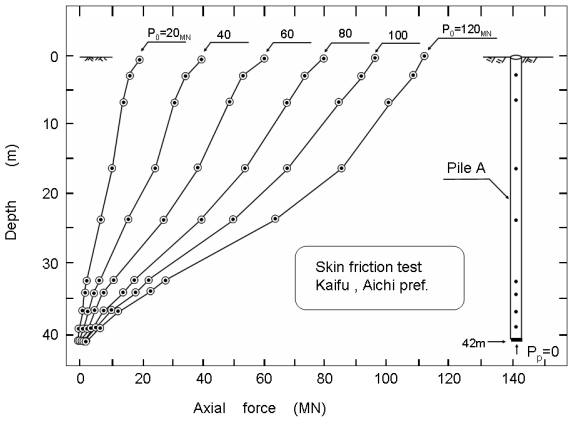

Figure 14. Distribution of the axial force versus depth in the skin friction tests at Kaifu (Ogura et al. 2005)

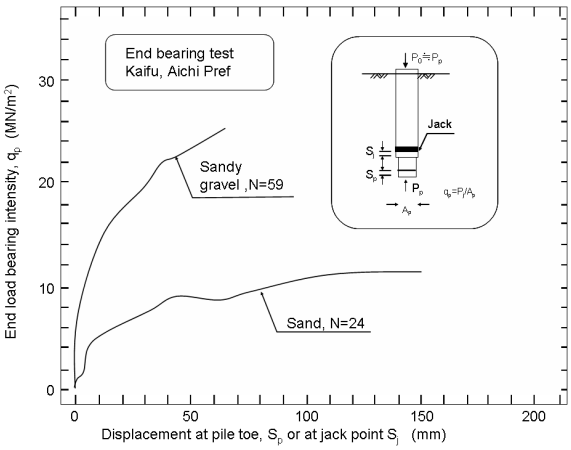

Figure 15. Displacement at pile toe, Sp or at jack point Sj versus end load intensity, qp (Ogura et al. 2005)

4. BEARING POWER OF BARRETTE PILE AS AGAINST CIRCULARPILE

The rectangular pile called Barrette pile has been of frequent use in recent years particularly for installing friction piles, because of its greater amount of shaft resistance that is mobilized in comparison with that of the circular pile. This effect is envisioned highly likely as the surface area on the shaft is apparently larger in the Barrette-type pile.

In order to verify this aspect, in-situ pile loading tests were conducted by Iwanaga et al. (1991) where the behaviour of the circular pile was compared to that of the rectangular pile having an identical cross sectional area. Shown in Fig. 16 is the layout of the two pile loading tests. The circular pile 1.2m in diameter had the same cross sectional area of 1.13m^2 as that of the 2.0×0.6m rectangular pile, but the latter had a surface area which was 1.38 times larger than that of the former. There were two sets of earth anchors as shown in Fig. 16 which were installed to carry reaction force when the load is applied on top of the piles. The test site was located at Tsukimino in Kanagawa Prefecture due west of Tokyo. The soil profile there is shown in Fig. 17 together with the side view of the two piles. There is a thick wind-blown deposit of clayey silt termed "Kanto loam" having the SPT N-value of the order of 5 to 30 to a depth of 14.5m. Below the loam layer, there exists a stiff sandy soil deposit of diluvial origin with the N-value in excess of 50. Two piles were installed by lowering the rebar cage into the prepared hole and concreted.

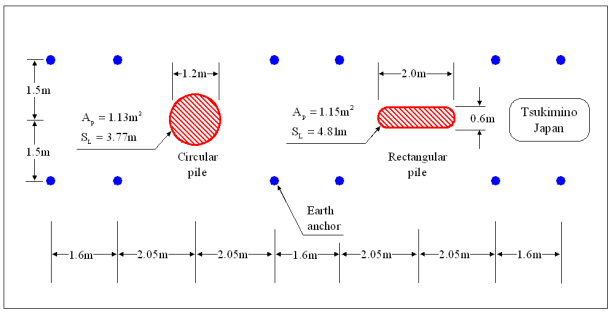

Figure 16. Layout of the pile loading tests, one on a circular and the other on a rectangular pile at Tsukimino (Iwanaga et al. 1991)

Strain gages were attached to the reinforcement cage of the piles to measure the axial load at several depths as shown in Fig. 17. The tests were of normal loading type in which the load Po is applied at the pile top and the settlement measured at the top.

The result of the pile top loading test on the circular pile is presented in Fig. 18 in which the pattern of the load-reload cycles is displayed versus time on the upper left-hand side. The progress of the settlement with time is shown on the lower left-hand side in Fig.18. On the basis of the time-changes thus obtained, the load-settlement curve in cyclic loading is established as shown in the lower right-hand side of the diagram. By reading off the maximum values of load and settlement at each cycle, the load-settlement curve was obtained as shown in the upper right-hand side.

The results of the pile top loading test on the rectangular pile is demonstrated in Fig. 19 in the same fashion as that of the loading test on the circular pile. Comparison of the load-settlement curves in the upper right-hand side of Figs. 18 and 19 does apparently indicate that the bearing power is greater for the rectangular pile than for the circular pile. To demonstrate this feature more vividly, the load-settlement curves for the circular pile and rectangular pile are shown together in Fig. 20. In Fig. 20 (a), the settlement, so, at the pile top is plotted versus the load, Po, at the pile top, where it can be clearly seen that the rectangular pile exhibited the ultimate bearing power of 17MN as against 13MN in the circular pile. The ratio of increase in the

bearing power in the Barrette pile is about 1.3 times as compared to the circular pile.

There were strain gauges equipped at the pile toe portion embedded through 2.5~3.0m into the stiff sand layer, as shown in Fig. 17. Based on the measured data, the equivalent axial force, Pp, mobilized by the friction at the portion of the pile toe was estimated. The force Pp divided by the area Ap at the toe is plotted versus the settlement at the pile tip Sp in Fig. 20 (b). The settlement Sp was taken approximately equal to that at the pile top So. As shown in Fig.ure 20 (b), the ultimate load intensity for the rectangular pile was 11MPA as against 8.6MPA in the circular pile. Thus, there was 1.24 times increase in the bearing power mainly by frictional resistance at he portion of the toe in the case of the rectangular pile. It is obvious that the increase has emerged from the fact that the rectangular pile (Barrette-type pile) has the larger surface area over which the frictional resistance at the toe portion can be mobilized, even if the cross sectional area is the same.

5.1 Outline of the Project and Construction

In-situ measurements of shaft resistance were carried out in the excavated shaft during the construction of cast-in-place reinforced concrete piles for the foundation of the United Overseas Building in Singapore (UOB). The 66-storey building 281m high was constructed in 1992 in the central business district of the city. As shown in Fig. 21, it is located on the right bank of Singapore River about 500m from its exit to the Marine Bay. The building as it stands now is shown in Fig. 22. The approximate soil profile in the east-west direction is displayed in Fig. 23 where it can be seen that there exits a marine clay deposit about 10~30m think overlaid by a surface fill and peaty clay layer. Below the marine clay, there is a residual soil deposit of medium stiffness which is underlaid by the bouldery clay. The layers of alluvial deposits above the bouldery clay are called Kallang Formation. According to the paper by Han et al. (1993), the bouldery clay deposit is composed of stiff to hard soil deposits interspersed with sandstone-derived boulders. The boulders varying in size and in shape from a few centimeters to 6m occupy about 20~30% of the total volume. Thus, the boulders are seldom in contact with each other. The soil/clay matrix behaves essentially as a stiff to hard, heavily over-consolidated clay and it tends to soften when put in contact with water. The undrained shear strength of the clay matrix as evaluated via the pressiometer test and plate loading test was shown to be about 1.0Mpa ≅ 10kgf/cm^2. The bouldery clay deposit is estimated to extend down to about 120m depth and the majority of high-rise buildings in the district are founded on the base structures constructed in this bouldery clay deposit as shown in Fig. 24. Construction of the foundation for the UOP Plaza is described somewhat in details by Iwanaga et al. (1991) and Imamura et al. (1991). The following is the excerpt from the reports.

The UOB plaza carrying a total weight of 1512MN was constructed on the foundation with 12 caissons supported by the shaft friction. The plan view of the layout of the foundation is demonstrated on the left side of Fig. 25. The right side indicates the portion of strutted excavation to construct the 5-storey podium attached to the high-rise tower.

The entire floor area of the building complex is enclosed by the diaphragm walls with a thickness 0.8m to 1.2m which was embedded to a depth of 15m to 40m where the competent residual soil or bouldery clay layer exists. The diaphragm walls were designed to act as the permanent walls for the 3-level basement car park. The side view of the caisson and bored piles along the cross section CA3 through CA6 is demonstrated in Fig. 26 where it can be seen that the upper part of the piles through soft alluvial deposits (Kallang Formation) consists of the caissons enclosed by the diaphragm walls. The lower part of the foundation was composed of the segment of cast-in-place reinforced concrete.

The method of constructing the caissons in the upper part consisted first in installing the diaphragm walls through water-saturated soft ground, as illustrated in Fig. 27. For the CA8-pile having an inner diameter of 7.6m, the diaphragm wall was constructed by following the three steps of cutting 1, 2 and 3 as illustrated in Fig. 27(c). By sealing off the groundwater and retaining the soil behind, excavation was advanced in dry conditions by machines. In the course of downward excavation, the reinforced concrete ring beams were constructed in-situ at an interval of 5~6m, to provide circular bracing for the diaphragm wall. When the excavation reached the level of the boulder clay deposit, that is, the toe of the diaphragm wall, the cutting was carried out further down in open conditions while protecting the exposed soil surface by placing the ring-shaped cast-in-place reinforced concreting circular segments 40cm thick and 2m wide.

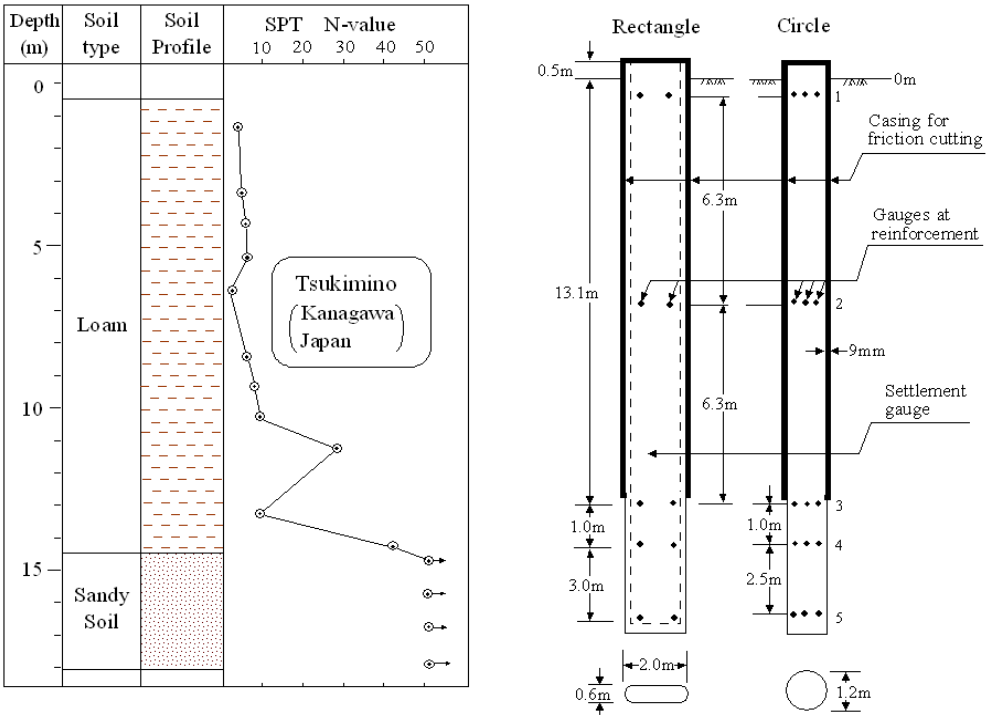

Figure 17. Soil profile and side view of the two piles (Iwanaga et al. 1991)

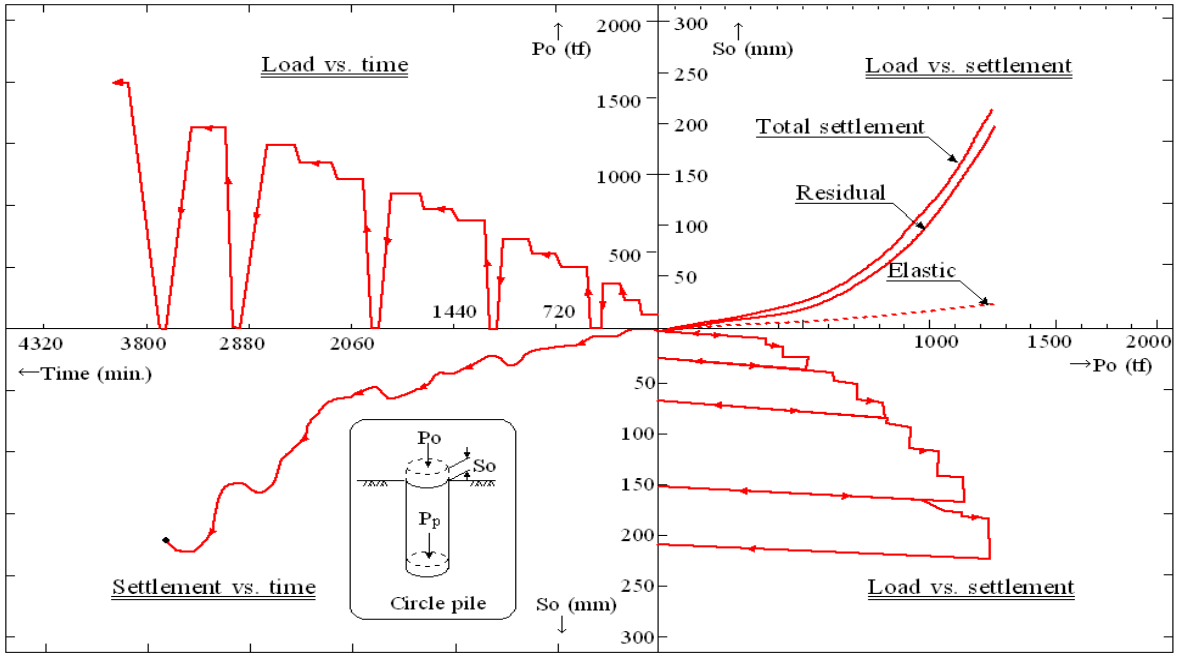

Figure 18. Load-settlement-time relations obtained by the pile top loading test on circular pile, Tsukimino, Kanagawa (Iwanaga et al. 1991)

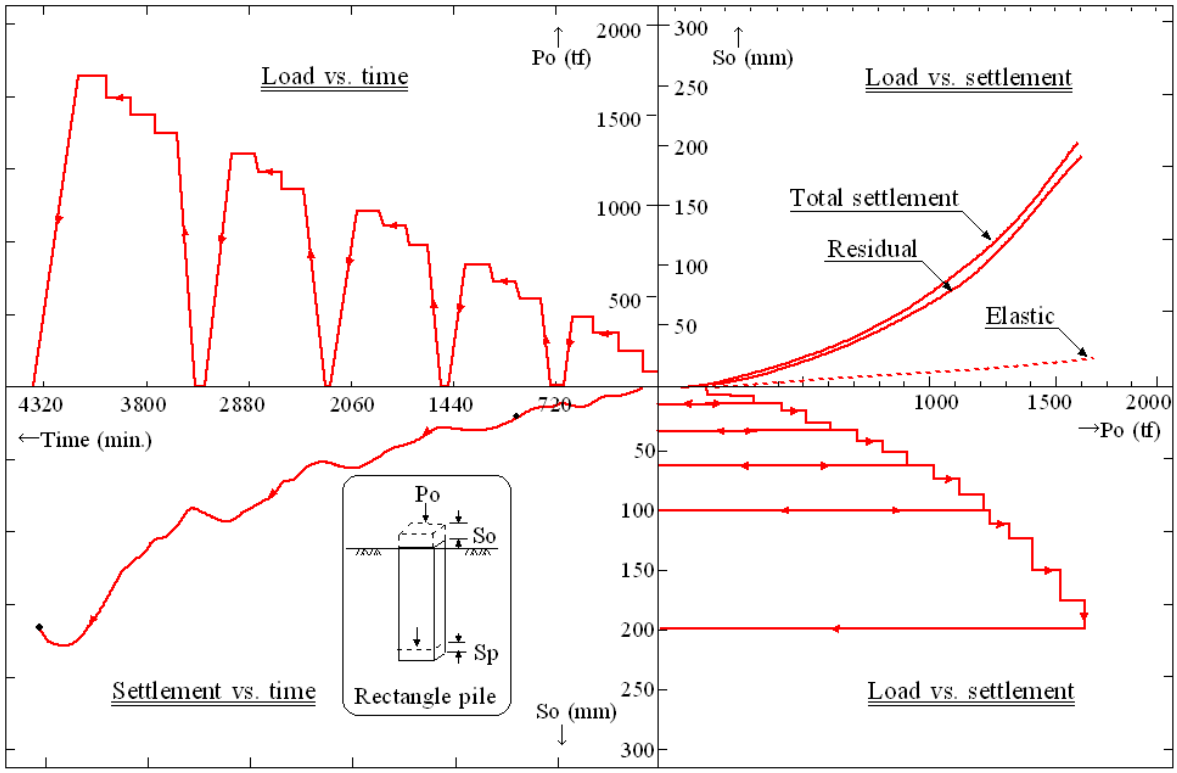

Figure 19. Load-settlement-time relations obtained by the pile top loading test on rectangular pile, Tsukimino, Kanagawa (Iwanaga et al. 1991)

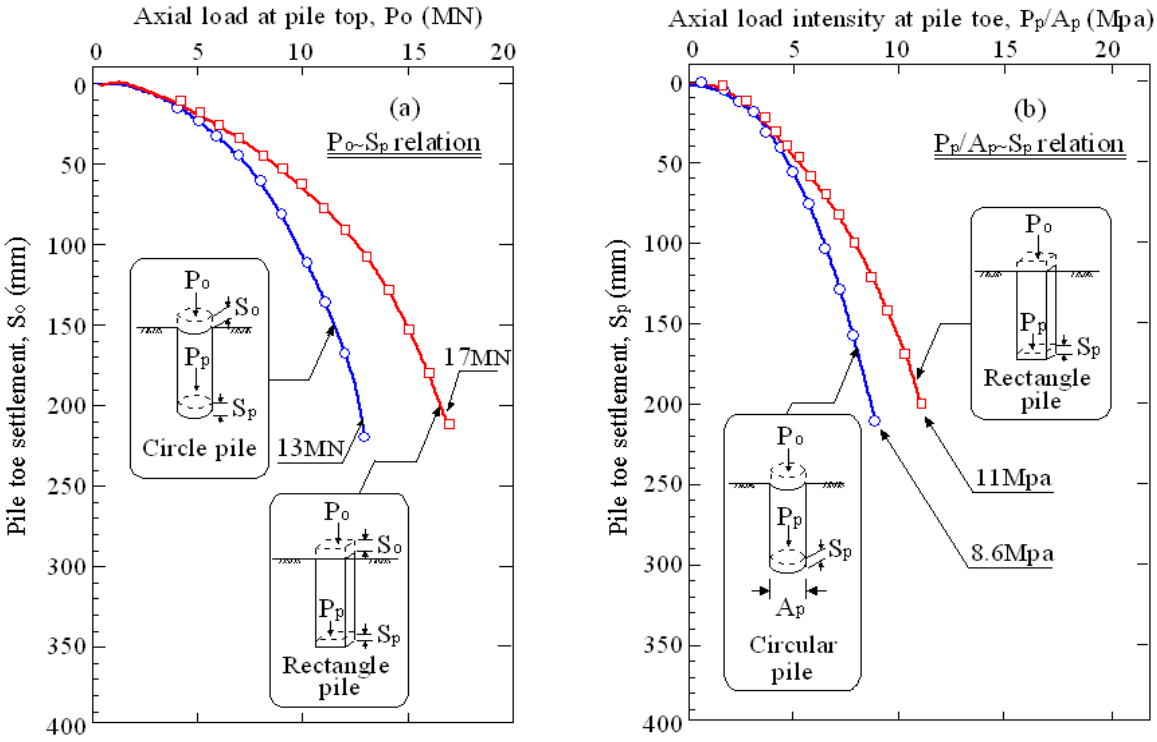

Figure 20. Load-settlement curves from the pile loading tests on the circular and rectangular piles at Tsukimino (Iwanaga et al. 1991)

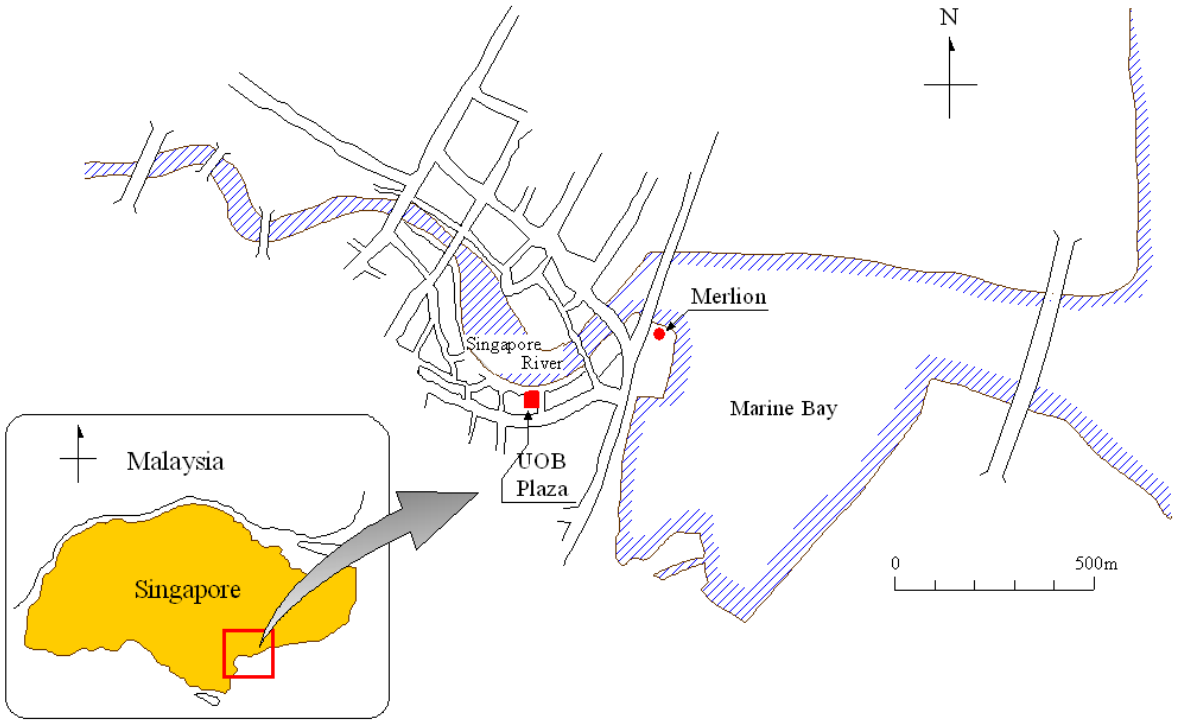

Figure 21. Location of UOB Plaza in Singapore

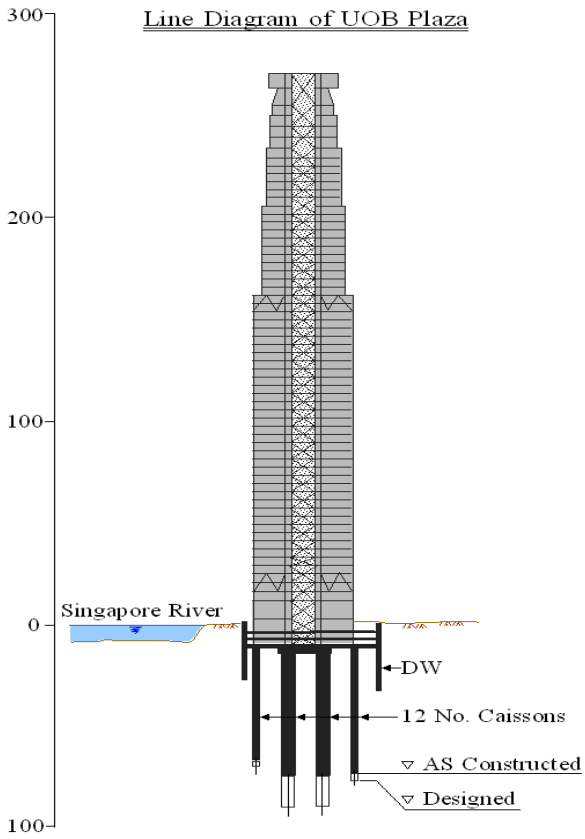

Figure 22. UOB Plaza in Singapore

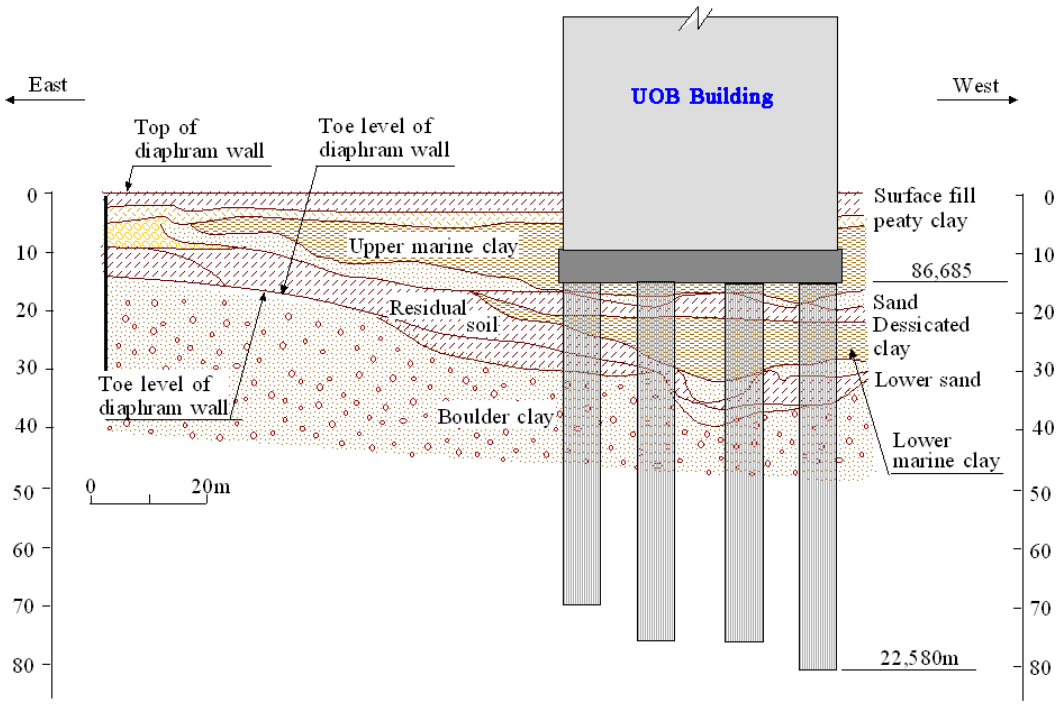

Figure 23. Site geology around the UOB Building in Singapore

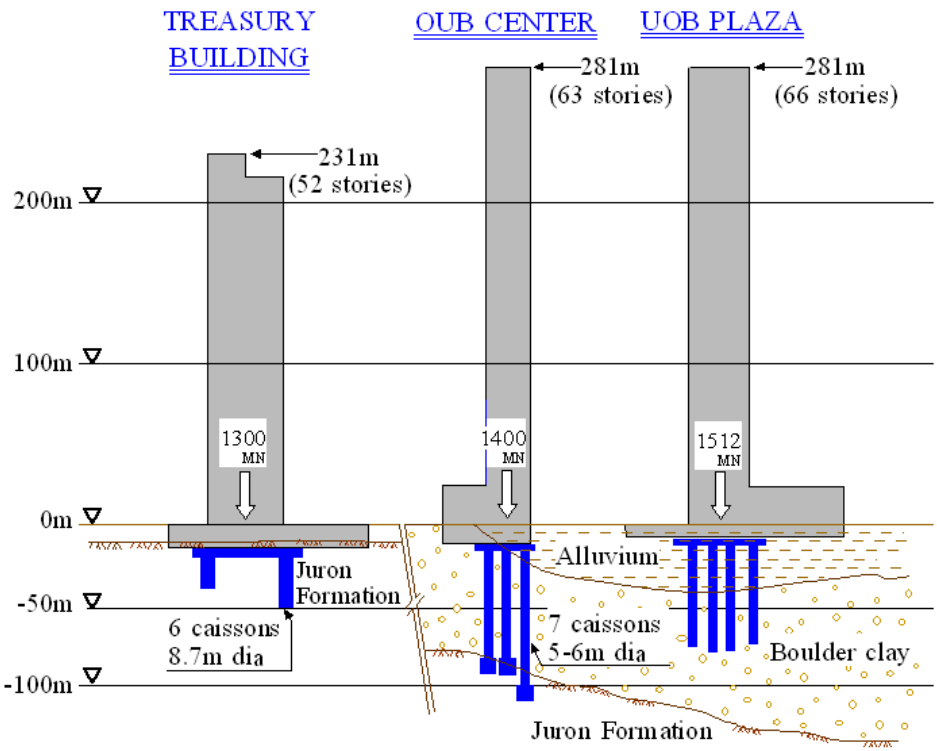

Figure 24. Typical features of building foundations in the central business district in Singapore

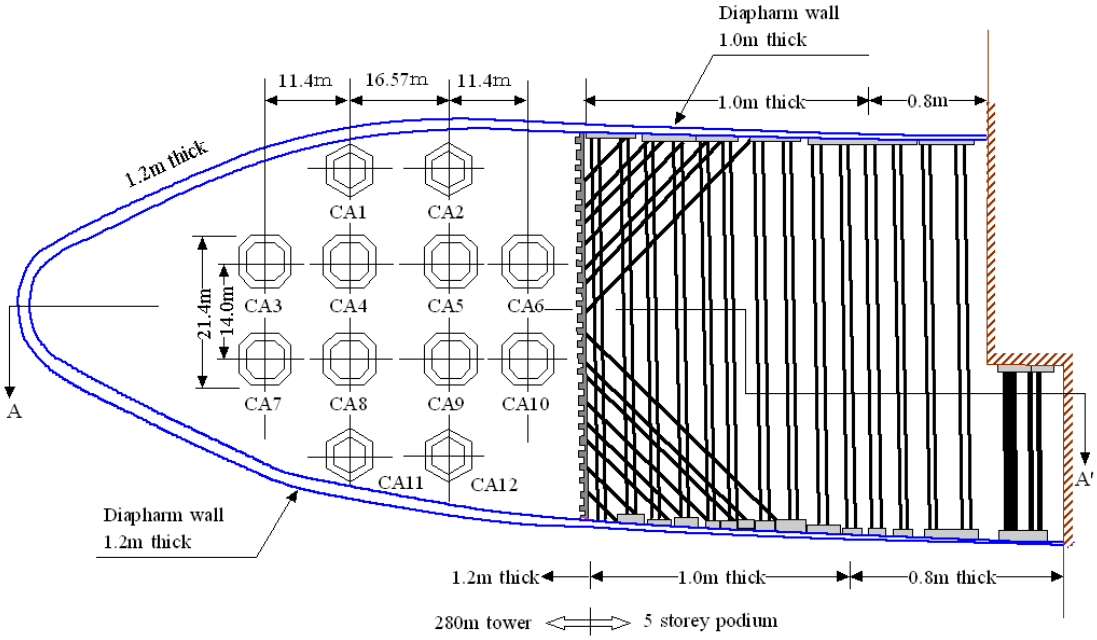

Figure 25. Layout of the bored piles for UOB Plaza

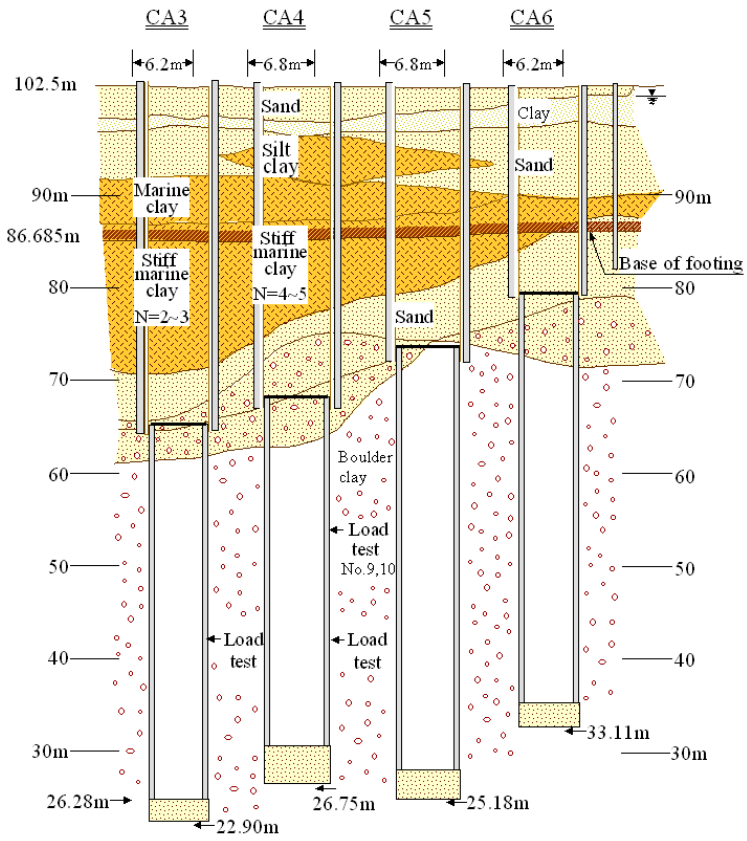

Figure 26. Layout of the caissons and bored piles for the UOB Plaza Building

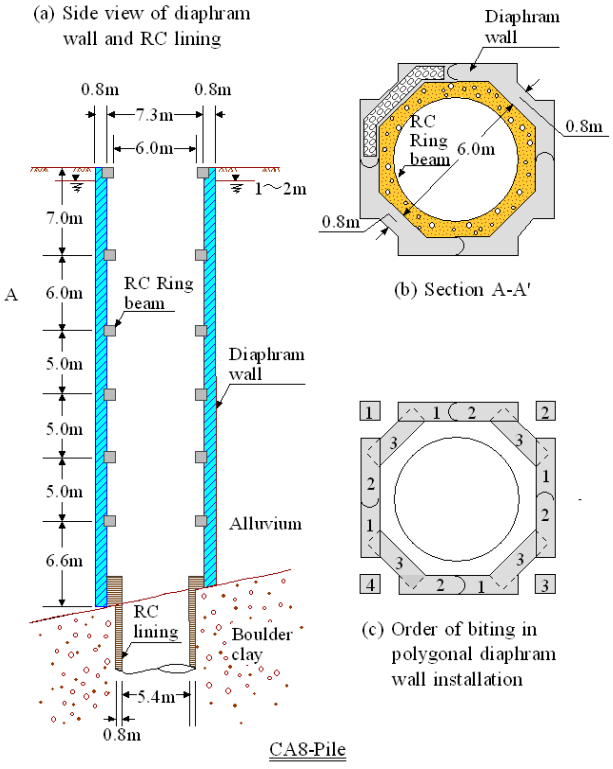

Figure 27. Construction of diaphragm walls and RC lining for foundations of UOB Building

5.2 In-Situ Measurements of the Shaft Resistance

As the excavation proceeded through the bouldery clay deposit, in-situ loading tests were performed at a total of 26 spots. The exact locations of the loading tests conducted in the shaft CA3 and CA4 are indicated in Fig. 26. The scheme of the loading test at the bottom of the current stage of excavation is schematically illustrated in Fig. 28. The lower segment B of the concrete wall to be tested had been constructed against the soil wall with an open gap 75cm wide on top of the bottom segment C. The upper segment A of the concrete ring for testing had also been constructed with an open gap of 75cm apart from the bottom of the already-constructed upper segment C.

Twelve hydraulically operated jacks were placed along the concave shelf in the annular space 80cm in height as illustrated in Fig. 28. The setup of the jacks along the circular shelf is shown somewhat in details in Fig. 29. Measurements of the vertical displacement were made during the jack-driven loading by means of several dial gauges as well as by means of the transit viewing apparatus, as illustrated in Fig. 28.

Some of the test results are demonstrated in Fig. 30 in terms of the total applied load plotted versus the measured displacement. Figure 30(a) shows the load-displacement curves obtained from the tests loaded upwards to No. 9 segment and downwards to No. 10 segment which were located at an elevation of 51m in the CA4 bored shaft, as accordingly shown in Fig. 26.

It may be seen that the ultimate skin friction mobilized between the concrete ring wall in 6.8m in diameter and surrounding bouldery clay deposit was 220tons=2.2MN for the segment No. 9 but for the segment No. 10 the ultimate friction would have been greater than this value. The results of the tests conducted at No. 4 and No. 5 segment in the bored shaft CA2 with the diameter of 4.7m are shown in Fig. 30(b), where it may be seen that the ultimate shaft friction was somewhere between 1.8 and 2.0MN. From the series of the loading tests as above, the ultimate value of the shaft resistance was obtained for the cast-in-place reinforced concrete segment which is installed in contact with the boulder clay in Singapore.

The outcome of the tests on 26 ring segments with the diameter of 4.7, 6.2 and 6.8m is summarized in Fig. 31 in terms

of the shaft resistance τ_f plotted versus depth. Fig. 31 shows that there is a tendency of increasing shaft friction with increasing diameter of the ring segment. However, looking over the entire test results, one can recognize that the ultimate value of shaft friction was in excess of 45tf/m^2. Based on the test data as verified above, the value of the ultimate skin friction used for the original design were modified from 45tf/m^2 to 35tf/m^2, which conduced greatly to reducing the cost of bored pile construction. As a result, the length of the bored pile was shortened, as accordingly indicated in Fig. 22.

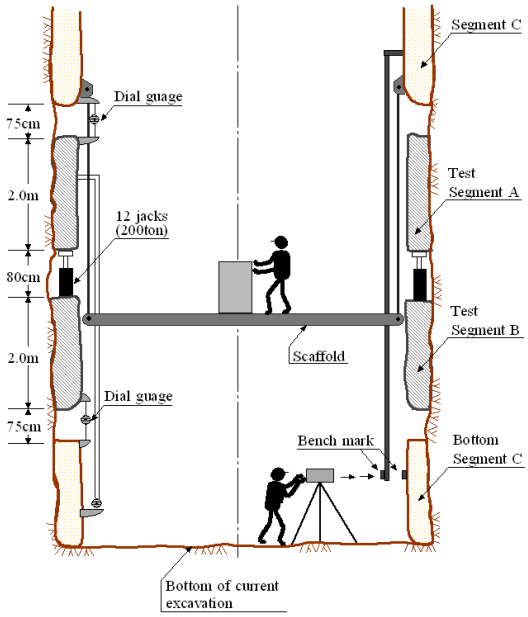

Figure 28. Scheme of the loading test for shaft resistance within the bored hole

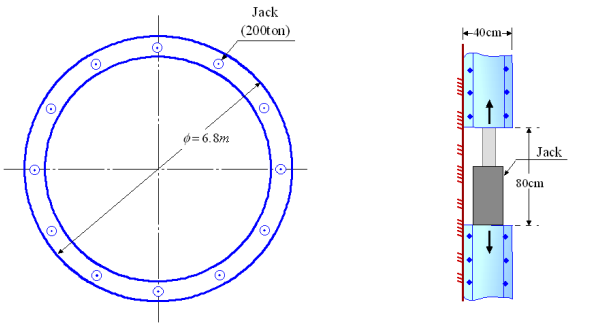

(a) Location of 12 jacks in plan for loading test

(b) Exact layout of the jack between two adjacent ring segments

Figure 29. Details of jack installation

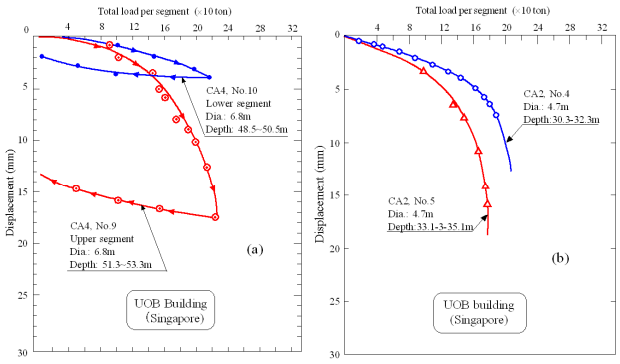

Figure 30. Load-displacement curves obtained from the in-situ loading tests

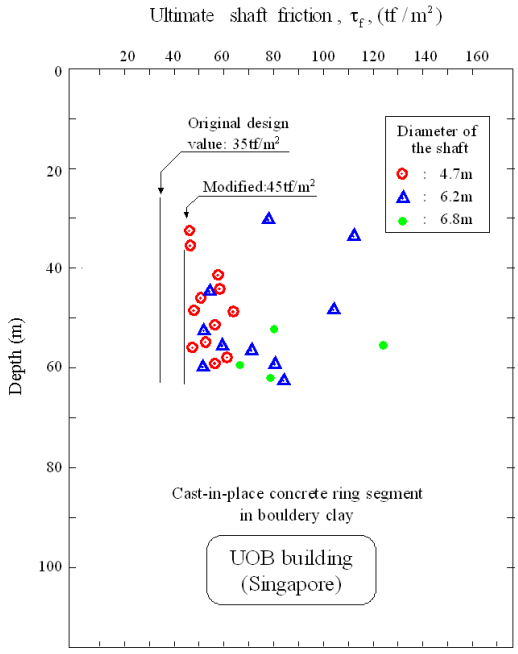

Figure 31. Ultimate shaft friction obtained from the in-situ loading tests

6. BEARING CAPACITY OF BORED PILES RELATED TO SPT N-VALUE

A vast majority of in-situ loading tests on bored piles ever performed in Japan was compiled and summarized in a form of charts in the Japanese design manual of building foundations (2001). These are shown in Figs. 32 and 33, where the ultimate toe bearing load intensity, P_f, and ultimate friction resistance, τ_f, are shown in terms of the plots against the SPT N-value. In the case of the toe resistance, it has been customary to take an average N-value over the 2m section, viz. 1m above and 1m below the tip level of piles. This averaged value is denoted by $\overline{N}$ and plotted in the abscissa of Fig. 32. In the case of the skin friction, the N-value at the depth of measurements is directly used in the abscissa as shown in Fig. 33 to represent the stiffness or strength of the soil materials surrounding the piles. Shown in Fig. 32 with black dots are the results of in-situ measurements on end bearing loads for the bored piles which were designed as friction piles.

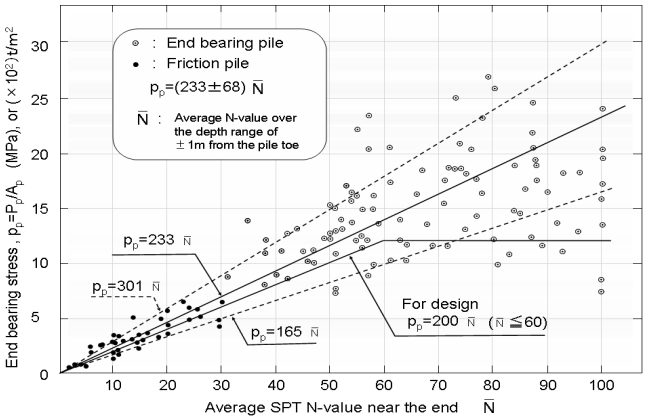

Figure 32. Summary plots of the ultimate toe bearing load intensity as function of averaged N-value (from Japanese manual)

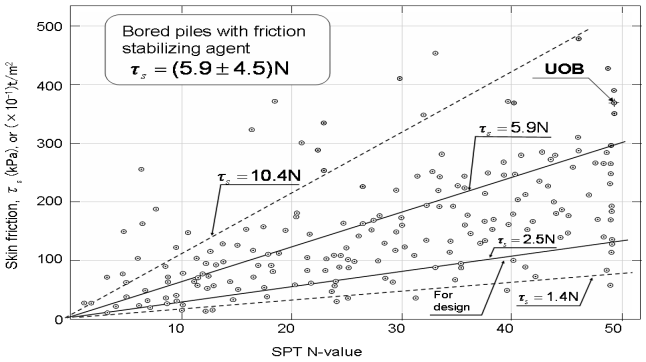

Figure 33. Summary plots of the ultimate skin friction as functions of SPT N-value (from Japanese manual)

Needless to say, the value of the point resistance is shown to be relatively small because the major part of the external load is carried by the skin friction. The data points indicated by open circles in Fig. 32 are those derived from the measurements on the bored piles designed as end bearing piles. Since the skin friction was not taken into account, the end bearing capacity does naturally take large values in excess of $P_f = 7\text{MN/m}^2$. Although there are considerable scatters in Fig. 32, an average line $P_f = 233\overline{N}$ is drawn through the cluster of data points, together with two other lines corresponding to the standard deviation of $\pm 30\%$. It is recommended in the manual that the relation $P_f = 200\overline{N}$ be used for design purpose for the deposits having a $\overline{N}$-value less than 60.

With respect to the ultimate skin friction plotted in Fig. 33 against the SPT N-value, there also are considerable scatters in the test data, but an average line $\tau_f = 5.9N$ is drawn through the cluster of data points, together with the $\pm 50\%$ lines of deviation. It is recommended in the manual that the relation $\tau_f = 2.5N$ be used for the design of the bored piles.

It is of interest to see where the result of the shaft friction tests in UOB building in Singapore is plotted in diagram of Fig. 33. Assuming that the N-value is greater than 50, the value of $\tau_f = 350\text{kPa} = 35\text{ton/m}^2$ is plotted in Fig. 33. It is observed that this value is located in the vicinity of the average line deduced from the Japanese case studies.

7. CIRCULAR DIAPHRAGM WALL FOR UNDERGROND STORAGE TANK

In early 1970 techniques have evolved extensively for liquefying natural gas and transporting it by ships over a long distance. The liquefied natural gas (LNG) carried to the site of destinations is once stored in a large tank. In response to demand it is transformed back into gas again and distributed for industrial or domestic use. In the wake of this trend, the construction of large-capacity storage tanks began in Japan in 1970's. In the early stage, the tanks were constructed on the ground, but for the sake of easiness of maintenance and safety as well attempts have been made to construct the tanks underground.

One of the early efforts in this context was the construction of the storage tanks in Sodegaura on the east coast of Tokyo Bay. The location is shown in Fig. 34. The tank was constructed in 1989 and had dimension 64m in diameter and 44m in depth with a storage capacity 170,000 kℓ. The bird-eye view of the roof of the tank is shown in Fig. 35 and its side view is displayed in Fig. 36, together with the soil profile. The critical issues for the design of the circular diaphragm wall were two-fold, viz., the thickness of the wall and the depth of its embedment.

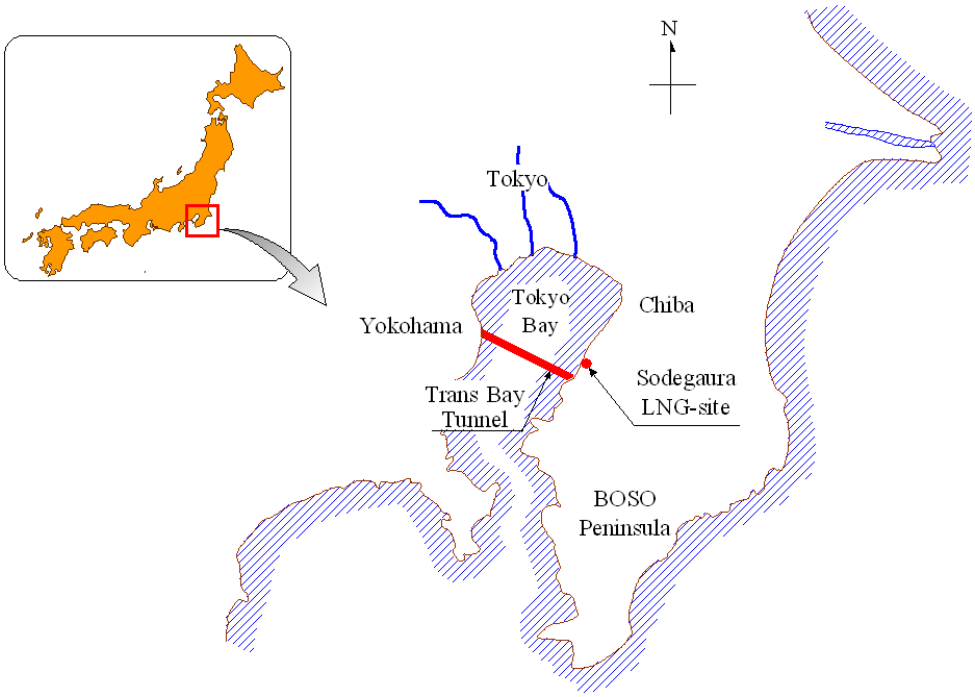

Figure 34. The location of the Trans Tokyo Bay Tunnel and LNG tanks

Figure 35. Underground LNG tank at Sodegaura, Chiba, Japan

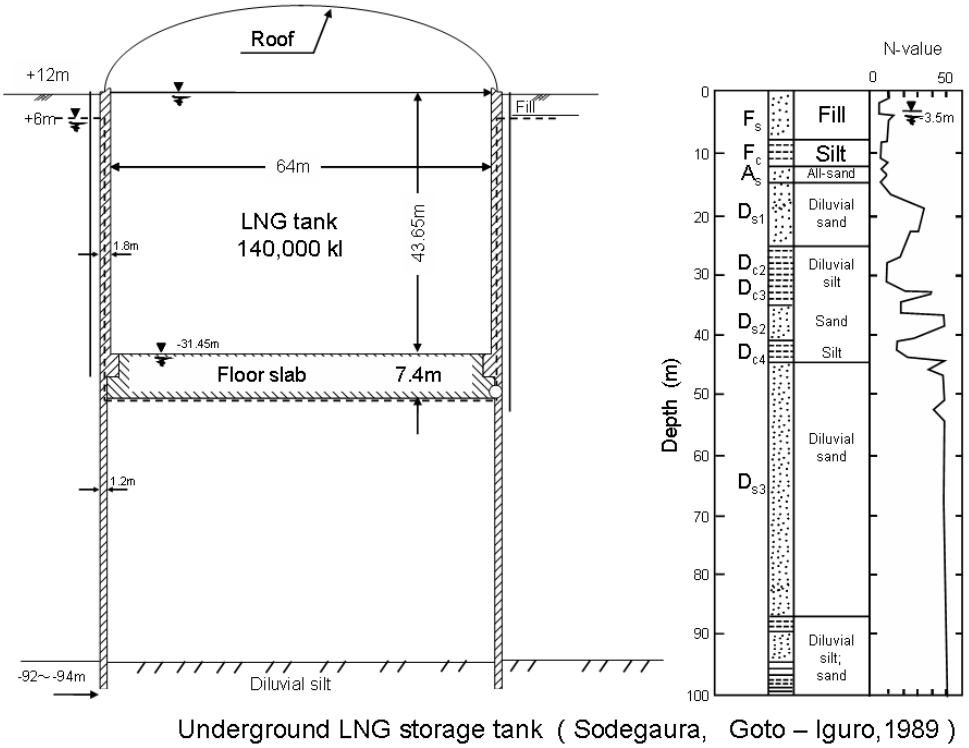

Figure. 36 Underground LNG storage tank at Sodegaura (Goto-Iguro, 1989)

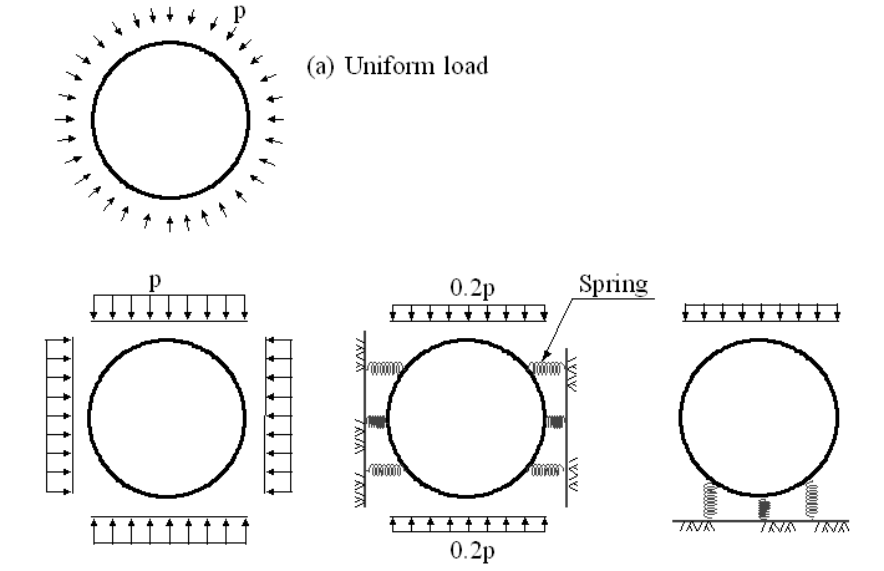

Figure 37. Three types of external loads in the design of the diaphragm wall

7.1 Wall Thickness

The thickness of the wall was determined by considering three kinds of external loads expected to act on the wall. The first is the uniformly distributed load directed to the center of the circle, as illustrated in Fig. 37(a), which is specified from the earth pressure at rest plus water pressure at each depth for which $K_o = 0.5$ was assumed. It is to be noticed that the effect of this uniform pressure is exactly the same as that of the equivalent uniform pressure acting from the four directions as shown in Fig. 37(b). Therefore, the uniform load as shown in Fig. 36 (b) is generally adopted for performing design calculation. The second load was the biased load acting from two directions as illustrated in Fig. 37(c). This kind of load is taken into account, because there always are some unidentified sources inducing eccentric load application such as sloped layers of underground deposits and non-uniformity of soil deposits. Since it is difficult, however, to estimate its magnitude, it was assumed to take a value 0.2 times the magnitude of the uniform load.

When the effects of earthquake loading are to be considered, the load from one direction is assumed to act as shown in Fig. 37(d). In the present case of the LNG tank, the magnitude of the earthquake force was assumed to be 0.15 times the uniform load. As a result of the load application as mentioned above, the thickness of the wall was determined to be 1.2m, although there are some differences in the reinforcement in the direction of the depth depending upon the computed bending moment in the body of the diaphragm wall.

7.2 Stability Check for the Uplift and Seepage

In carrying out excavation in the dry condition, it is a common practice to lower the ground water table inside to a level 1-2m below the bottom of the excavation. The ground water table below the impervious layer is lowered outside the diaphragm wall to a degree necessary for reducing the uplift water pressure acting at the bottom. Anyway, the most critical time is at the final stage of excavation as shown in Fig. 38. Considering this stage, stability check is generally made by comparing the total weight of soil-water mass in the portion AA'BB' with the uplift water pressure at the bottom which is equal to $\gamma_w \ell (D/2)^2 \pi$. It is usual to control the water table level inside or outside of the excavation so that the factor of safety of at least about 1.03m can be maintained. The stability check for seepage-induced piping may need to be made by comparing the hydraulic gradient against its critical value. Since it is difficult, however, to evaluate the critical value, the general practice is to design the diaphragm wall so that its toe can penetrate deep enough through an impervious layer with sufficient thickness.

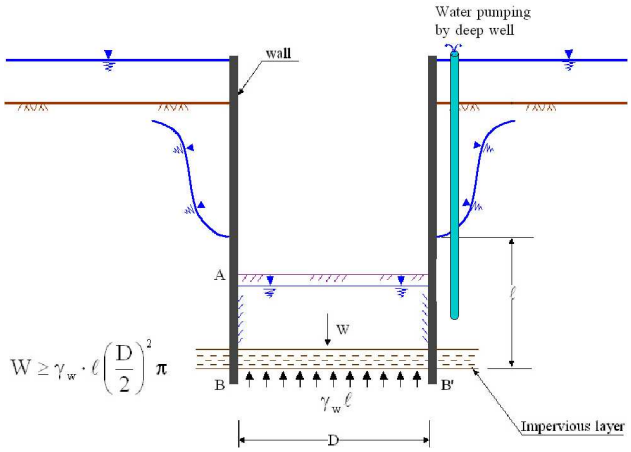

Figure 38. Stability against bottom uplift

7.3 Method of Excavating Ditches

While there are several methods which are different in details and in size, the method for excavating ditches for the diaphragm wall can be roughly classified into two groups as described below.

7.4 Rebar Lapping Method

The steps for constructing the wall are illustrated in Fig. 39. First of all, rectangular ditches are excavated by a cutting machine for the A-element (advance element) at a certain interval as shown in Step 1. Drilling mud is filled in the ditch at this stage. Then, reinforcement cage (rebar cage) franked by two long steel plates is lowered into the mud-filled ditch and concrete is cast by tremie pipe. At this time, the steel plate tends to be deformed outward due to the weight of un-cemented concrete.

To prevent this, it is common to throw gravels or crushed stones into the space outside the steel plates as illustrated by Step 2 in Fig. 39. Then, the excavation is made for the element B (follow element). In this case, both ends of the Section A are still filled with gravels, but gravels are excavated together and the

bottom is cleaned up as shown in Step 3. Since the concrete at the element A has already been solidified, there is no extra pressure acting on the steel plate to induce its deformation. After the excavation, the rebar cage is lowered into the mud and concrete is poured as illustrated in Step 4. Note that the rebar in Section B is assembled so that it can fit well at both ends to the already existing reinforcements projecting from the side of element A.

When this method is adopted, the cutting of the ditch is made generally by using the machine as shown in Fig. 41. The axis of the cutting bit is arranged vertically and by rotating the bit horizontally, the excavation can be advanced at the bottom. Since the connection between element A and B is very tight, this method is adopted for constructing diaphragm to be used as permanent structure.

7.5 Concrete Cutting Method

As illustrated in Step 1 in Fig. 40, the ditch excavation is carried out at element A at a certain interval. Then, the rebar cage without the steel plates is lowered and concrete is poured as shown in Step 2. When the B-element is excavated in the next stage, the cutting is performed not only for the portion of soils but also for the hard portion of concrete on both sides, as illustrated in Step 3. Then, installation of the rebar and concreting is carried out as shown in Step 4. When using this method, the ditch is excavated by means of the machine having the horizontal two-axes of cutting bit. The two cutting bit is rotated horizontally in mutually opposite directions so that the bit can cut the surround soils upwards on both walls. A typical machine is shown in the photograph later in Fig. 49. This concrete cutting method is adopted for constructing the diaphragm wall used for temporary retaining structure, and also for the case of circular walls where the hoop compression is expected to induce high compressive loads in the circumferential direction. In the LNG storage tank, the rebar lapping method was used, because the diaphragm wall was intended to function as permanent structure. No matter whichever method is adopted, the same method can be applied for the circular-shaped wall construction as well. It is to be noted that what is called circular wall is not exactly the round circle. It has a multi-angular shape.

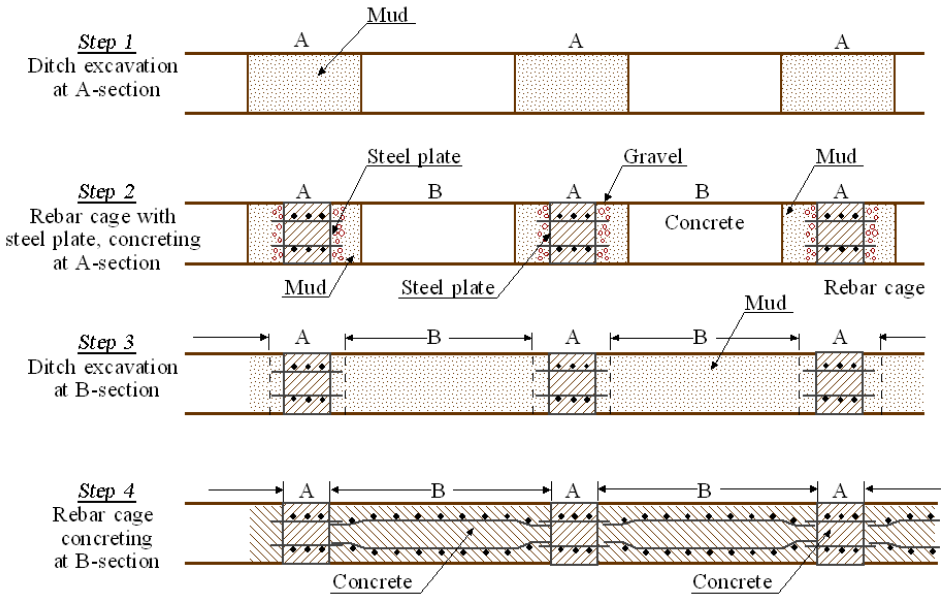

Figure 39. Diaphragm wall by rebar lapping method

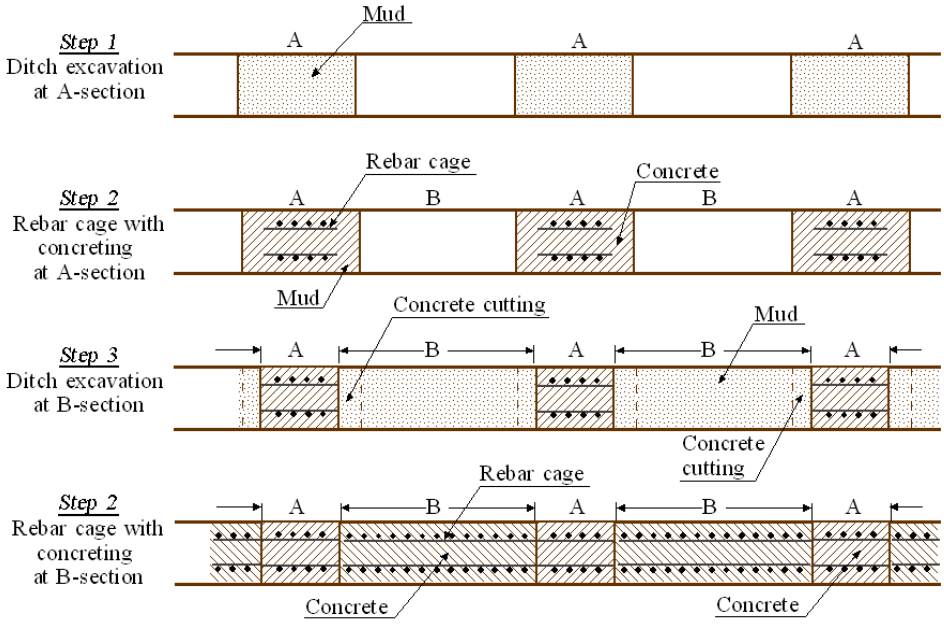

Figure 40. Diaphragm wall by concrete cutting method

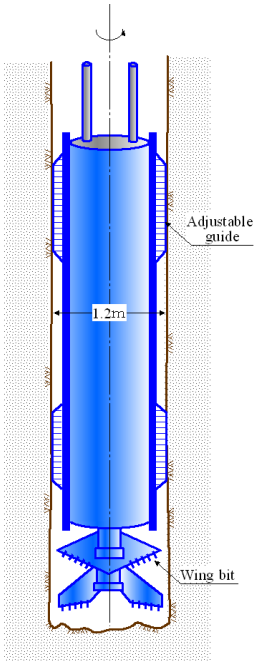

Figure 41. Cutting machine for the ditch

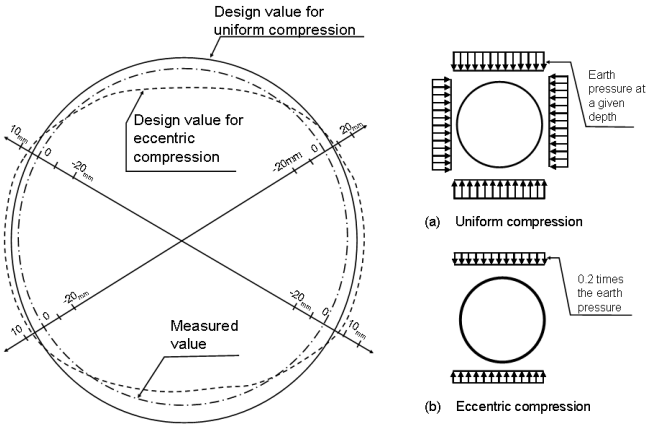

Figure 42. Design loads and measured wall displacements in radial direction, LNG storage tank at Sodegaura (Goto-Iguro, 1989)

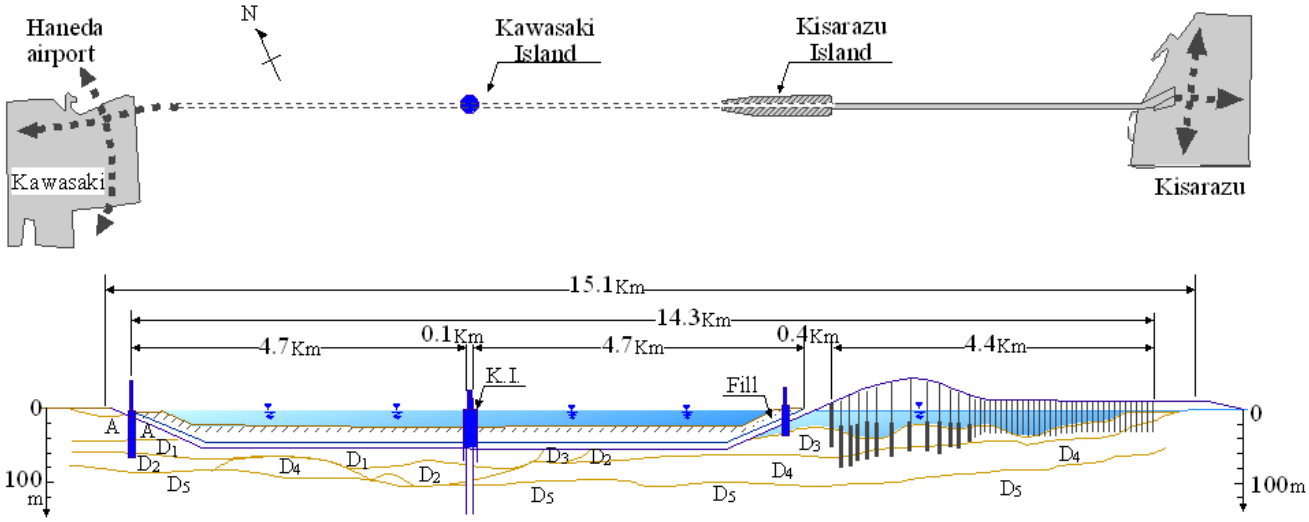

Figure 43. Plan and side view of the trans Tokyo Bay tunnel

7.6 Observed Performances

The measurements were made of the earth pressure and lateral wall deflection at several points around the circular diaphragm wall after the construction of the LNG tank at Sodegaura site. Shown by the solid line in Fig. 42 is the already deflected feature of the wall top as computed using the uniform design load in Fig. 37(b). Although the amount of deflection is not shown explicitly, it was of the order of 1cm. Needless to say, the deflection was uniform and, hence, the solid line is a true circle. The dotted line in Fig. 42 indicates the deviation of computed wall deflection by considering the eccentric design load shown in Fig. 37(c).

The dotted line in Fig. 42 indicates the deviation of computed wall deflection by considering the eccentric design load shown in Fig. 37(c). It is apparent that the deflected shape is slightly oval. The chain-dotted line in Fig. 42 shows the lateral deflection of the wall top actually measured at the time when the excavation had been completed to the targeted depth. It may be seen in Fig. 42 that the measured distribution of the wall lies within the two lines of deflection computed using the design loads indicated in the right hand of the figure.

8. LARGE DIAPHRAG WALL AT KAWASAKI ISLAND IN TRAINS TOKYO-BAY UNDERSEA TUNNEL

8. 1 General

The Trans Tokyo-Bay tunnel connecting Kawasaki city on the west and Kisarazu city on the east was constructed during the period of 1989-1997 to provide the 4-lane highway across the Tokyo Bay. The location of the highway is shown in Fig. 34. Out of the 15km long highway, the eastern and the undersea tunnel with a diameter of 14m was constructed for the 10km long stretch on the west as shown in Fig. 43. In the middle of the tunnel, a man-made island called Kawasaki Island was constructed to provide a starter base for launching the shield tunnel to the east and to the west. This island was intended to be equipped with a facility for ventilation when the highway traffic is in service. Since the Island was to be located in the middle of the sea and seated in the soft soil seabed at a water depth of 28m, the greatest challenge was posed for its safe construction. A series of steps taken for constructing the diaphragm wall and

some difficulties encountered will be described below somewhat in details.

8. 2 Soil Conditions in Seabed

The soil conditions at the site were investigated by two deep borings drilled to a depth of 135m from the sea level. The outcome of this investigation is displayed in Fig. 44. It can be seen that there exists a soft silty clay deposit (AC_1) of alluvial origin with the SPT N=0 to a depth of about 22m from the sea bottom which is underlaid by a series of alternate layers of sand and silt of diluvial origin down further to a depth of about 45m from the sea bottom. Below this the deposits consist mainly of stiff soils with N-values in excess of 50. Since the diaphragm wall had to be embedded to a sound base deposit through sufficiently impervious clay or silt layer, of most critical concern was the decision as to how deep the diaphragm was to be penetrated. The presence of the impervious layers with sufficient thickness and stiffness is demonstrated in Fig. 45.

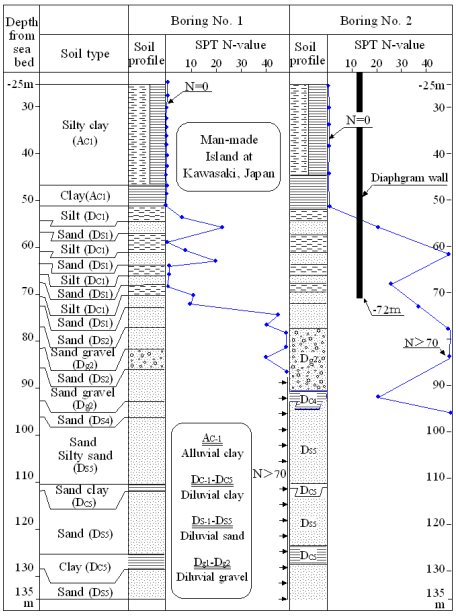

Figure 44. Soil profiles at the site of Kawasaki Island

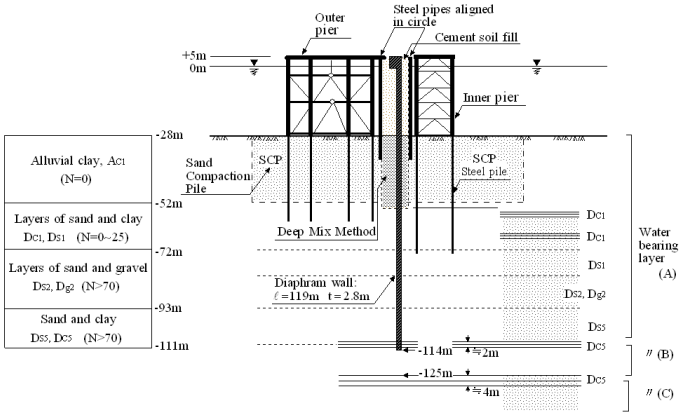

Figure 45. Soil profile and water-bearing layers at Kawasaki Island

8.3 Construction of the Diaphragm Wall

The sequence of the process for constructing the Island consisted of several steps as illustrated in Fig. 46. In this case, the concrete cutting method illustrated in Fig. 40 was adopted.

(1) First of all, the soft clay and soft deposits under the seabed were stabilized to a depth of 35m below the seabed by the method called sand compaction pile (SCP) over the circular area about 120m in diameter. The area ratio of compaction was 30% and 78.5% in plan. The compaction pile was constructed by means of the heavy machinery equipped on board the ship. The annual portion of the seabed deposit with an inner diameter of 100m was stabilized by the Deep Mixing Method (DMM) in which the soft soils were churned and mixed with cement to improve these into somewhat stiff materials. The zones of SCP and DMM are indicated in Fig. 46(a).

(2) After the work of soil stabilization was over, steel pipe piles 1,016m in diameter were driven by the hammer-operated machines aboard the ship to provide the foundation for the jacket structure to be put into place later on. The jacket frame unit assembled at the yard at other site was carried by a tug boat and its legs were put on the top of the pile. One of the jacket frame units in the yard is shown in Fig. 47. The feature of the jacket unit sitting at the site of the Island is displayed in Fig. 46(b). The pier thus constructed was used as the working platform for further work of diaphragm construction and excavation.

(3) The jacket-type platform consisted of three circular piers with two outer piers connected with each other by the flat floor at the top. This is called outer pier and the other one inside is called inside pier. The next step was to drive a number of steel pipes 40cm in diameter side by side in contact in a circular alignment along the outside rim of the inner pier and also along the inside rim of the outer pier. The circular arrangement of the pipes along the inside of the outer pier is shown in the plan view of Fig. 48(a). After constructing two circular walls in this way by driving pipes side by side, the annular space 12.6m wide between these two walls was filled up by dumping cement-mixed soils from the pier. It is to be noted that the seabed deposit just underneath the soil-cement fill had been stabilized by the technique called Deep Mixing Method (DMM). The feature of this phase of construction is illustrated in Fig. 48(c).

(4) From the top floor of the pier platform, excavation was advanced downwards through the 12.6m wide cement-mixed soil fill and further down to a depth of 119m from the floor level of the pier. Excavation was carried out by what is called the reverse circulation method using the two-axes rotating type cutting bits as shown in Fig. 49. The width and length of one element of excavation was 2.8m and 2.35m, respectively. Special caution was taken to maintain the in-plumb condition of excavated shaft within an accuracy of 1/1000 by using a high-precision apparatus. The circular diaphragm wall had an outer diameter of 103.6m and a total length of 119m counted from the working platform on the pier. Rebar cages were lowered unit by unit and concrete was poured in the bored holes. This phase of the construction is illustrated in Fig. 46(d).

(5) After installing the circular diaphragm walls with a width of 2.8m, sea water inside the enclosed wall was pumped out and excavation was advanced to the level of -72m below the sea level within the diaphragm wall while lowering the ground water level. The dewatering and control of the water table level inside and outside the diaphragm wall during the excavation was conducted by means of two sets of deep wells as illustrated in Fig. 50. One is the well points to pump water up from the two water-bearing pervious layers designated as A and B in the figure. The other set was installed within the excavated pit to observe the level of water during excavation. The still other was to observe the ground water level at the deepest layer C. The levels of water table indicated in Fig. 50 are the targeted level for the final stage of excavation down to the floor at the depth of -72m. It is to be noticed that the design and control of the water tables are the most critical issue in the challenge of deep excavations below the natural ground water table. The

excavation was advanced to a targeted level and then framed structure of the inner jacket was dismantled and removed. The circular row of the pipes was also taken away together with the cement-mixed soil to expose the inside surface of the diaphragm wall. This phase of the construction work is schematically illustrated in Fig. 46(e). When the excavation reached the level of -28m, a huge ring-shaped hoop composed of 6 reinforced concrete blocks 5.8m thick and 11m high was installed around the inside periphery of the diaphragm wall. This was intended to assure the tightness of the junction between blocks in the formation of the wall. The feature of this installation is shown by a picture in Fig. 48. The platform of the bird-eye view is shown in Fig. 52.

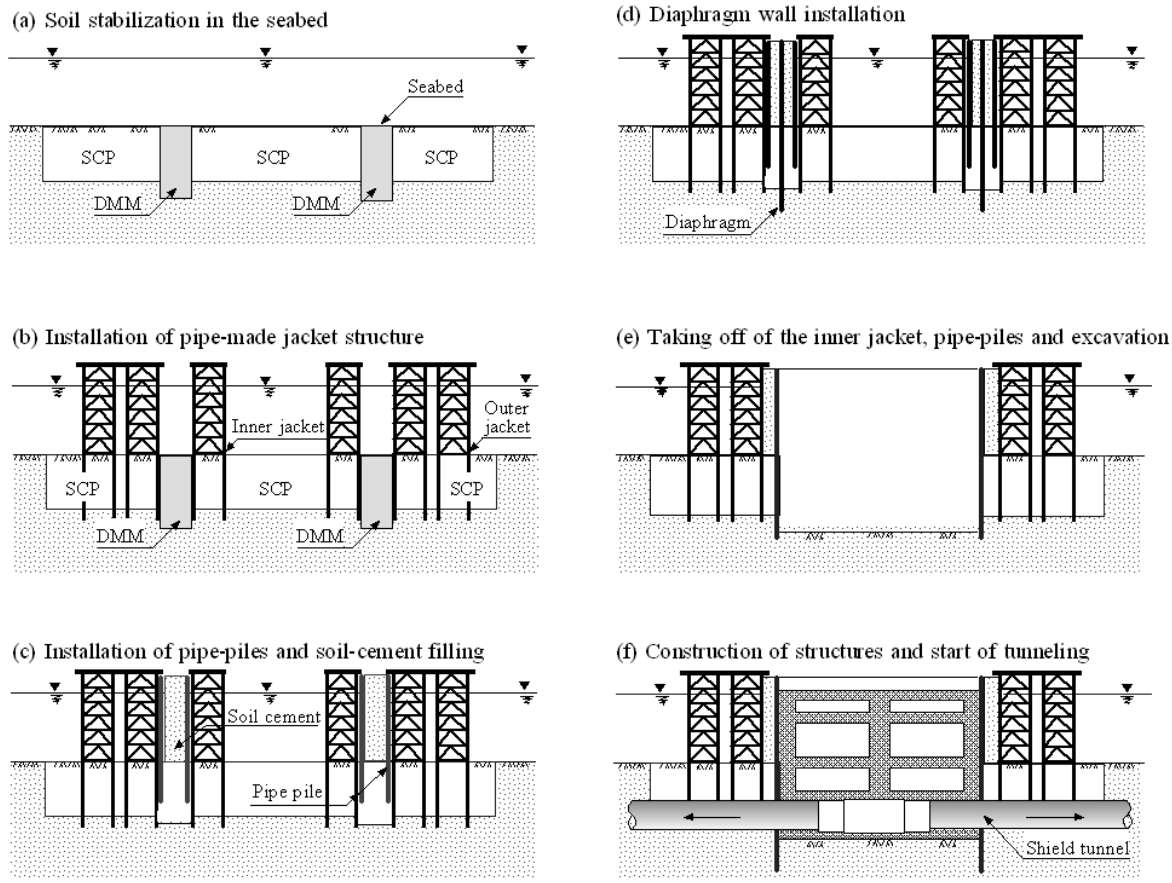

Figure 46. Construction process of the manmade Island

Figure 47. Unit of jacket frame sitting on the assembling yard

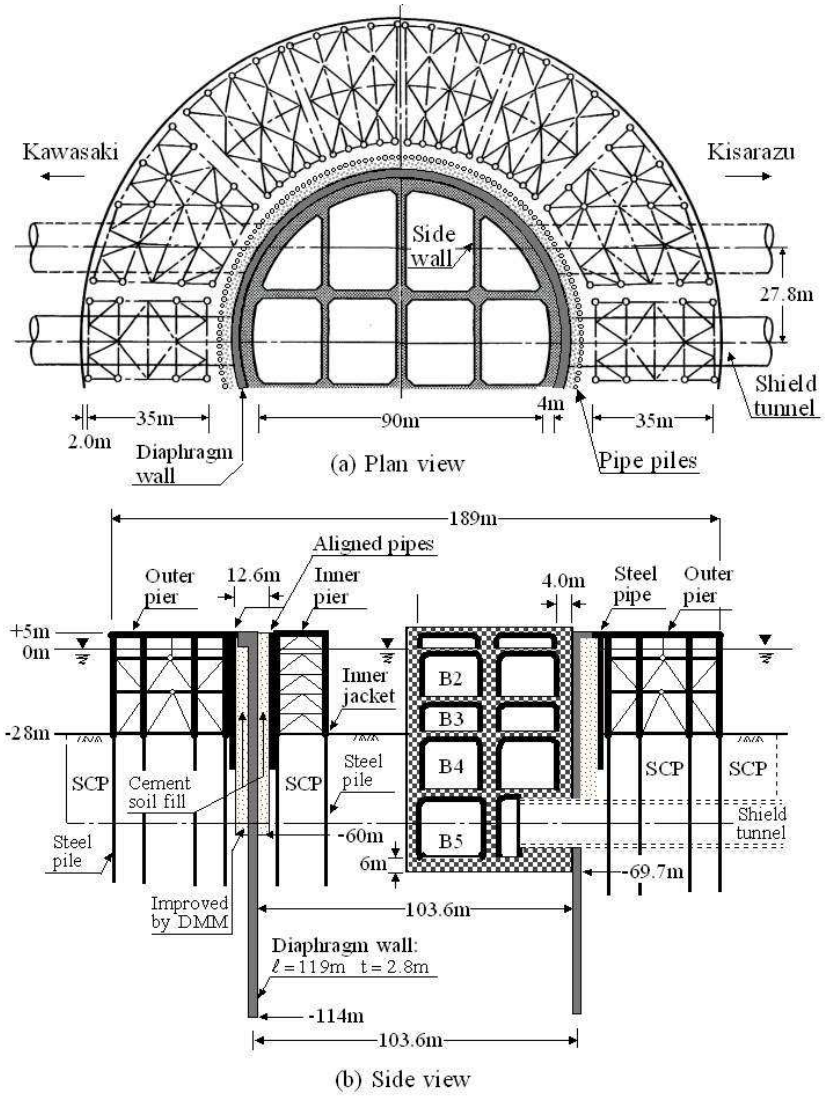

Figure 48. Layout of the platform and piers in Kawasaki Island

Figure 49. Two-axes rotating type cutting bits

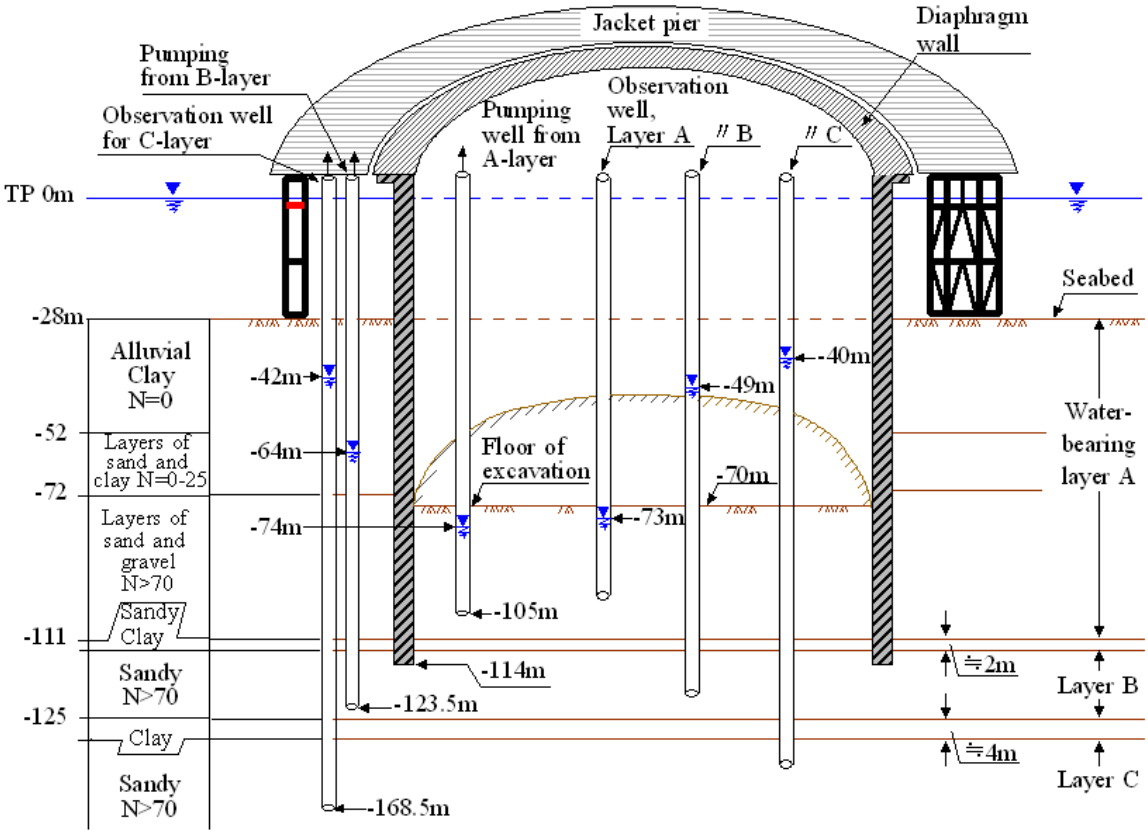

Figure 50. Observation and control of water levels inside and outside of the excavated pit

Figure 51. Installation of a block hoop at the depth of -28m

Figure 52. Bird-eye views of the platform of the piers

8.4 Performances of the Diaphragm Wall

There were two important items to be considered in the structural design of the circular diaphragm wall. One was the earth pressure acting on the wall and the other was the force in circumstantial direction which acts as support to maintain the stability of the wall. As there was no bracing structure inside the wall, it was considered of utmost importance to make sure whether the hoop compression was uniformly transmitted in the circumferential direction, not causing any deviation. There are two aspects to be paid attention in discussing design and performance of the circular diaphragm wall.

1) In the upper part of the wall, distribution of the hoop load, earth pressure and wall deflection around the circle is an important factor, because any significant deviation is associated with a risk of eccentricity of the overall behaviour.
2) In the lower part of the wall, a great magnitude of compressive stress is induced in the circumferential direction. Therefore, a special concrete with high compressive strength ought to be cast. In the Kawasaki Island, the strength of the concrete was specified as 36MN/m^2.

In order to monitor the performances of the diaphragm walls, several set of strain gages were attached to the rebar cages. Also, the earth pressure cells and tilt meters were installed in the wall before concrete was cast. Figure 53 shows the circumferential compressive stress measured in the walls at three stages of excavation.

When the inside excavation reached the level of -28m, a huge ring-shaped hoop was installed as indicated in Fig. 53(a). At this stage, the hoop load monitored at three locations was distributed versus depth as shown in Fig. 53(a) with its maximum value of about 20MN/m occurring at the depth of 80m. As the thickness of the wall was 2.8m, this maximum corresponds to 20/2.8=7.14MN/m^2 in terms of load intensity. Shown in Fig. 53 (b) is the depthwise distribution of the circumferential load per 1m depth at the stage when the excavation had progressed to the level of 40.4m. It is noted that the maximum load of about 38MN/m was monitored at the floor level of excavation, viz., at the depth of 40.4m. The distribution of the circumferential load per 1m depth at the near-final stage of 69.7m deep excavation is demonstrated in Fig. 53(c), where it is noted that the maximum load was about 40MN/m occurring at the bottom level of excavation. This corresponds to a compressive load intensity of 40/2.8=14.3MN/m^2=143kg/cm^2 which is apparently smaller than the compressive strength of the concrete, 36MN/m^2, used in the design of the diaphragm wall. One of the features to be noticed is the variation of the hoop load amongst three points of measurements along the periphery, particularly at shallow depths. It is noted in Fig. 53 that the variation was not so significant, indicating no likelihood of buckling-type deformation to take place along the periphery of the diaphragm wall due to eccentricity of the load distribution. At greater depths, the compressive stress itself is an important factor. The measured stress was shown to be lower than the strength of 36MN/m^2 which was achieved with the use of high-strength concrete.

At the time the design was made, analyses were made to evaluate the compressive stress in the hoop direction. The results of the analyses are also indicated in Fig. 53. On the basis of the analysis results, the design load was specified reflecting the records of previous cases of diaphragm construction. The load distribution thus determined for the design of Kawasaki Island is also indicated in Fig. 53. In view of the good coincidence with the analysis and design values, actual progress of the excavation was considered satisfactory and to have been executed successfully.

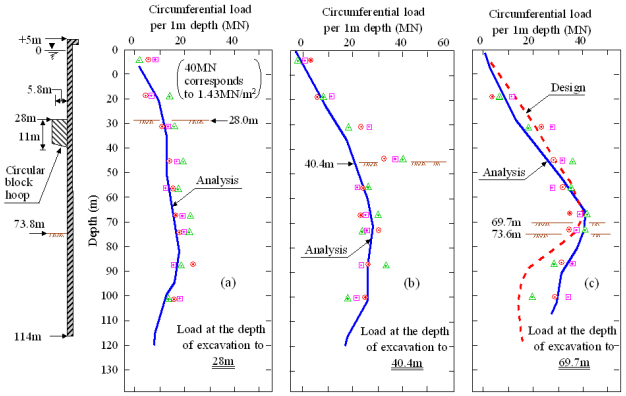

Figure 53. Distribution of the circumferential load intensity versus depth

The external force acting on the diaphragm wall was the earth pressure and water pressure from inside and outside as well of the wall. The earth pressure was measured by means of the pressure cells buried at various depths at four locations around the wall. The results of measurements are shown in Fig. 54 where it may seen that the earth pressure acting on the outer face of the wall (Fig. 54(b)) was, by and large, smaller than that evaluated by the theory assuming Ko=0.5. The earth pressure on the inside of the wall was somewhat scattered and took values in excess of those evaluated by theory at two depths. However, in the deeply embedded portion, the larger earth pressure tends to act to make the wall safer against the heaving of the excavated bottom, and therefore, it was considered not to cause any serious problem. Distribution of measured horizontal inward displacements is shown in Fig. 55, along with the values corrected for the effects of temperature. It can be seen that, at the stage of excavation to the depth of 69.7m, the maximum wall deflection was of the order of 2cm and that occurred at the bottom of the excavation. The displacement of this order of magnitude was judged as acceptable for safe performance of the diaphragm wall.

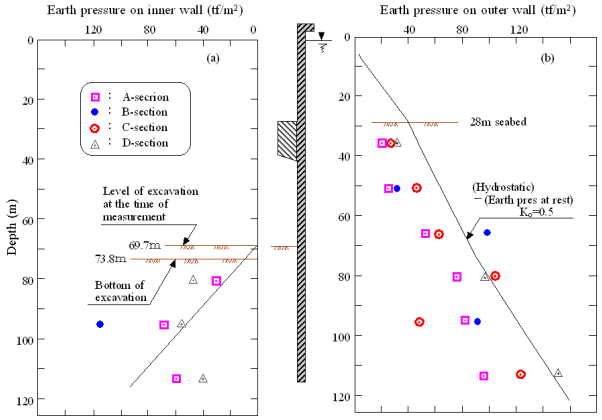

Figure 54. Measured earth pressures at two locations at the stage of excavation to the depth of 28m

8. CONCLUDING REMARKS

In a majority of cases of foundation design in Japan, it is possible to locate a stiff layer in the deposits of dense sand, gravel or soft rocks at depths 20-50m where a sufficient bearing capacity can be obtained. In view of a certain degree of uncertainty in assessing the skin friction, the piles are generally designed as the end bearing pile for which more reliance can be put for supporting superstructures. Under such circumstances, verification of the load carrying capacity of a given stiff layer as to whether it can indeed mobilize the design-assumed bearing capacity has been the major motivation to perform the in-situ pile loading tests.

As a consequence of a majority of the loading tests over the last two decades, fairly reliable sets of data have been obtained and accumulated. These are put forward in the manual published by the Japan Association of Architecture for the design and construction of buildings having 20 to 50 storeys.

For large structures such as bridges or dams, caissons or diaphragm walls are often used as foundations to support superstructures. In such cases, loading tests are generally carried out within excavated shafts or pits by applying loads directly to the intact surface of stiff soil or rocks. When the bearing layer is too deep or too difficult to designate such as the case of UOB building in Singapore, friction piles are planned and implemented, but verification of the bearing capacity by means of the in-situ tests become prerequisite. As a result of the loading tests, the pile length was reduced and this contributed greatly to the saving of the cost.

Diaphragm walls have been used for various purposes as temporary supports or as a part of main permanent structures. It is utilized to retain the soil ground for executing excavation to construct basements of buildings, subway stations, storage tanks etc. When the diaphragm wall is constructed in the form of straight line in plan for the purpose of water-proofness, precaution should be taken for tight connection at joints between two neighbouring elements. The structural design is made to resist against the earth pressure at rest plus water pressure acting from behind. Bracing system is always necessary in this case.

When the diaphragm wall is utilized in the form of circular-shaped retaining walls, more important is the hoop compression in the circumferential direction and eccentricity in the radial deflection. Since the hoop compression tends to increase with depth, it is a common practice to use high-strength concrete at deeper portions.

In this paper, the case of the LNG storage tank in Tokyo Bay was taken up to highlight issues of importance as above. The second example is the construction of the Kawasaki Island in Tokyo Bay. This is unique in the sense that it has the largest-ever depth of embedment and that it was constructed in the middle of the waters. In terms of the scale and the hurdles encountered, it may be cited as one of the most difficult unprecedented challenge in the recent history of civil engineering practice.

ACKNOWLEDGEMENTS

In preparing this text, information on the pile testing in Japan was given by Dr. H. Ogura, Technical director of Japan Pile Co. The test data on the UOB plaza and the prototype tests in Tsukimino were offered by Dr. T. Hosoi, former executive director of Nishimatsu Co. and by Mr. Y. Ueda at Singapore office of Nishimatsu Co. The information on the diaphragm construction at Kawasaki Island was offered by Kajima Co. and also by Dr. H. Yoshida, Vice-president of Chemical Grout Co. in Tokyo. Dr. T. Sueoka, director of engineering center of Taisei Co. also provided information on construction of the Kawasaki Island. Dr. S. Goto, former executive director of Tokyo Gas Co., kindly provided detailed account of the construction of the LGN storage tanks in Sodegaura. The author wishes to extend his sincere thanks to these experts mentioned above who furnished the most valuable information without which the writing of this text would not have been materialized.

This paper was originally submitted and printed in the Proceedings of the Bangladesh Geotechnical Conference (BGC-2009) held in Dhaka in December 2009. The author wishes to express his deep thanks to Professor A.M.M. Safiullah for giving his permission to publish this paper again in this journal in its present form.

9. REFERENCES

Goto, S. and Takahashi, Y. (1981), "Construction of Large LNG Inground Storage Tanks at Sodegaura Terminal," Tsuchi to Kiso," Vol. 29, No. 1, pp. 24-28. (in Japanese)

Goto, S. and Iguro, M. (1989), " The World's First High-strength, Super-Deep Slurry Wall," Proc. of the 12th International Conference on Soil Mechanics and Foundation Engineering, Rio de Janeiro, Vol. 2, pp. 1487-1490.

Han K.K., Wong K.S. and Broms, B.B. (1993), "Singapore Bouldery Clay: The Origin, Properties and Load Tests of Bored and Cast-in-Place Piles," Proc. 11th Southeast Asian Geotechnical Conference, Singapore, pp. 523-527.

Ho, C.E. and Wallace, J.C. (1993), "Design and Performance of Diaphragm Walls for a Deep Basement in Singapore," Proc. 11th Southeast Asian Geotechnical Conference, Singapore, pp. 715-720.

Iwanaga, K., Hirano, T., Ishii, T., and Ueno, T. (1991), "Considerations for Earth Pressure on Shaft and Pile Loading Test Rearranging, Nishimatsu Technical Research Report, Vol. 14, pp. 108-116. (in Japanese)

Japan Society of Architecture and Buildings, (2001), Manual of Recommendations for Design of Building Foundations, pp. 211-216.

Kishida, H. and Tsubakihara, Y. (1993), "An Analytical Method for Predicting the Displacement of a Pile and Soil Layers," Proc, 11th Southeast Asian Geotechnical Conference, Singapore.

Osterberg, J.O. (1984), "A New Simplified Method for Load Testing Drilled Shafts," ADSC, pp. 9-11.

Ogura, H., Sugai, K., Kishida, H. and Yoshifuku, T. (1995), "Application of the Results of Pile Toe Loading Tests on Evaluation of Behaviour of Cast-in-Place Concrete and Pre-Cast Piles", Tsuchi to Kiso, Japanese Geotechnical Society, Vol. 43, No. 5, pp.84-89. (in Japanese)

Ogura, H., Shibuya, T., Karkee, M.B. and Saito, M. (1997), "Toe Load Test on Large Diameter Cast-in-Place Pile for the New Building of Kanto Regional Postal Services Bureau, Part 2-Analysis and Interpretation of Results," Proc. 32nd Annual Convention of the Japanese Geotechnical Society, Saitama City, pp. 1433-1434. (in Japanese)

Ogura, H. and Shibuya (1998), "Toe Load Test on Large Diameter Cast-in-Place Piles", Kisoko, pp. 84-89. (in Japanese)

Ogura, H., Kuwayama, S., Suzuki, Y. and Yamamori, S. (2005), "Toe Bearing Resistance Test and Shaft Resistance Test on Large Diameter Bored Precast Pile", Proc. Annual Convention of Japanese Geotechnical Society. (in Japanese)

Photo Album "Tokyo Wan Aqua-Line" (1998), Japan Highway Public Corporation, and Trans-Tokyo Bay Highway Corporation.

Shibuya, T., Ogura, H., Kawamura, A. and Senno, H. (1997), "Toe Load Test on Large Diameter Cast-in-place Pile for the New Building of Kanto Regional Postal Services Bereau, Part 1 – Load Test Plan and the Results." Proc. 32nd Annual Convention of the Japanese Geotechnical Society, Saitama City, pp. 1431-1432. (in Japanese)

Imamura, M., Hosoi, T., Kado, Y. and Ishii, T. (1991), "Construction of Deep and Large-Diameter Caisson Type Piles", Journal of Japan Society of Civil Engineers, Vol.-14, No. 427, pp. 289-298.